



Fehr, M. A., Hammond, S. J., & Parkinson, I. J. (2018). Tellurium stable isotope fractionation in chondritic meteorites and some terrestrial samples. *Geochimica et Cosmochimica Acta*, 222, 17-33.
<https://doi.org/10.1016/j.gca.2017.10.010>

Peer reviewed version

Link to published version (if available):
[10.1016/j.gca.2017.10.010](https://doi.org/10.1016/j.gca.2017.10.010)

[Link to publication record in Explore Bristol Research](#)
PDF-document

This is the author accepted manuscript (AAM). The final published version (version of record) is available online via ELSEVIER at <http://www.sciencedirect.com/science/article/pii/S0016703717306737#ak005>. Please refer to any applicable terms of use of the publisher.

University of Bristol - Explore Bristol Research

General rights

This document is made available in accordance with publisher policies. Please cite only the published version using the reference above. Full terms of use are available:
<http://www.bristol.ac.uk/pure/about/ebr-terms>

1 **Tellurium stable isotope fractionation in chondritic**
2 **meteorites and some terrestrial samples**

3
4 Manuela A. Fehr^{1,2*}, Samantha J. Hammond¹, and Ian J. Parkinson^{1,3}

5
6
7 ¹ Department of Environment, Earth and Ecosystems, Centre for Earth, Planetary, Space &
8 Astronomical Research, The Open University, Walton Hall, Milton Keynes MK7 6AA, UK

9 ² Institute of Geochemistry and Petrology, ETH Zürich, 8092 Zürich, Switzerland

10 ³ Bristol Isotope Group, School of Earth Sciences, University of Bristol, Wills Memorial
11 Building, BS8 1RJ, UK

12
13
14 submitted to *Geochimica et Cosmochimica Acta* on 12th April 2017,

15 revised version

16
17 * Corresponding author: Institute of Geochemistry and Petrology, ETH Zürich,
18 Clausiusstrasse 25, 8092 Zürich, Switzerland; e-mail: manuela.fehr@erdw.ethz.ch; phone:

19 +41 44 632 89 16; fax: +41 44 632 11 79

24 **ABSTRACT**

25

26 New methodologies employing a ^{125}Te - ^{128}Te double-spike were developed and
27 applied to obtain high precision mass-dependent tellurium stable isotope data for chondritic
28 meteorites and some terrestrial samples by multiple-collector inductively coupled plasma
29 mass spectrometry. Analyses of standard solutions produce Te stable isotope data with a long-
30 term reproducibility (2SD) of 0.064 ‰ for $\delta^{130/125}\text{Te}$. Carbonaceous and enstatite chondrites
31 display a range in $\delta^{130/125}\text{Te}$ of 0.9‰ (0.2‰ amu⁻¹) in their Te stable isotope signature,
32 whereas ordinary chondrites present larger Te stable isotope fractionation, in particular for
33 unequilibrated ordinary chondrites, with an overall variation of 6.3‰ for $\delta^{130/125}\text{Te}$ (1.3‰
34 amu⁻¹). Tellurium stable isotope variations in ordinary chondrites display no correlation with
35 Te contents or metamorphic grade. The large Te stable isotope fractionation in ordinary
36 chondrites is likely caused by evaporation and condensation processes during metamorphism
37 in the meteorite parent bodies, as has been suggested for other moderately and highly volatile
38 elements displaying similar isotope fractionation. Alternatively, they might represent a
39 nebular signature or could have been produced during chondrule formation.

40 Enstatite chondrites display slightly more negative $\delta^{130/125}\text{Te}$ compared to
41 carbonaceous chondrites and equilibrated ordinary chondrites. Small differences in the Te
42 stable isotope composition are also present within carbonaceous chondrites and increase in the
43 order CV-CO-CM-CI. These Te isotope variations within carbonaceous chondrites may be
44 due to mixing of components that have distinct Te isotope signatures reflecting Te stable
45 isotope fractionation in the early solar system or on the parent bodies and potentially small so-
46 far unresolvable nucleosynthetic isotope anomalies of up to 0.27 ‰. The Te stable isotope
47 data of carbonaceous and enstatite chondrites displays a general correlation with the oxidation
48 state and hence might provide a record of the nebular formation environment.

49 The Te stable isotope fractionation of the carbonaceous chondrites CI and CM (and
50 CO potentially) overlap within uncertainty with data for terrestrial Te standard solutions,
51 sediments and ore samples. Assuming the silicate Earth displays similar Te isotope
52 fractionation as the studied terrestrial samples, the data indicate that the late veneer might
53 have been delivered by material similar to CI or CM (or possibly) CO carbonaceous
54 chondrites in terms of Te isotope composition.

55 Nine terrestrial samples display resolvable Te stable isotope fractionation of 0.85 and
56 0.60‰ for $\delta^{130/125}\text{Te}$ for sediment and USGS geochemical exploration reference samples,
57 respectively. Tellurium isotopes therefore have the potential to become a new geochemical
58 sedimentary proxy, as well as a proxy for ore-exploration.

59

60 **1. INTRODUCTION**

61

62 Tellurium (Te) is a chalcophile and siderophile element that is moderately volatile
63 with a 50% condensation temperature (T_c) of 709 K similar to that of Zn (726 K) and Sn (704
64 K) (Lodders, 2003). Experimental data suggests that Te partitions strongly into the Earth's
65 core (Rose-Weston et al., 2009), and therefore, it was suggested that a large portion of Te in
66 the silicate Earth originates from the late veneer (Rose-Weston et al., 2009; Yi et al., 2000)
67 consisting potentially of CI or CM carbonaceous chondrite-like material based on Se/Te ratios
68 (Wang and Becker, 2013). However, the near-chondritic Se/Te ratio of the mantle may not be
69 a primitive mantle signature, as has been suggested by (König et al., 2014). The isotope
70 signature of Te in chondrites and in the terrestrial mantle is therefore expected to provide
71 further constraints on the composition of the late veneer (Rouxel et al., 2002).

72 Non-traditional stable isotope fractionation data provide important information about
73 the formation of the solar system, early solar system processes and the evolution of planetary
74 bodies (e.g., Georg et al., 2007; Pogge von Strandmann et al., 2011; Poitrasson et al., 2004),

75 but Te stable isotope fractionation has scarcely been investigated. Terrestrial Te-rich ore
76 minerals display significant fractionation of Te of 2‰ in $\delta^{130/125}\text{Te}$ (Fornadel et al., 2017;
77 Fornadel et al., 2014; Smithers and Krouse, 1968). Experimental data further demonstrates
78 that abiotic and biotic redox processes can cause Te stable isotope variations (Baesman et al.,
79 2007; Smithers and Krouse, 1968). Liquid-liquid extraction can induce both mass dependent
80 (up to 1.9‰ in $\delta^{130/125}\text{Te}$) and mass independent Te isotope fractionation (Moynier et
81 al., 2008). In bulk meteorites, no mass-independent Te isotope variations are present
82 indicating that the early solar system was well mixed and homogenous with respect to Te
83 isotopes (Fehr et al., 2005). The study by Fehr et al. (2005) also derived low precision Te
84 stable isotope fractionation data, and data for one sample, the unequilibrated ordinary
85 chondrite Mezö-Madaras, indicated the possible presence of volatility induced fractionation
86 of Te by evaporation and/or condensation processes during metamorphism. Ordinary
87 chondrites display isotope fractionation for a series of moderately and highly volatile
88 elements such as Ag, Rb, Zn and Cd that was most likely produced by metamorphic processes
89 on the meteorite parent body (Luck et al., 2005; Nebel et al., 2011; Schönbacher et al., 2008;
90 Wombacher et al., 2008; Wombacher et al., 2003).

91 We have developed a new double spike procedure to obtain high precision Te stable
92 isotope fractionation data of chondritic meteorites and some terrestrial samples. These high
93 precision Te isotope analyses will be used to determine if metamorphic processes cause
94 volatility related fractionation of Te in ordinary chondrites. Additionally, we will investigate
95 whether Te stable isotope fractionation has the potential to elucidate the origin of moderately
96 and volatile elements on Earth and the nature of a potential late veneer addition by exploring
97 whether compositional differences exist between different chondritic meteorite classes for Te
98 isotopes.

99

100 **2. SAMPLES**

101
102
103
104
105
106
107
108
109
110
111
112
113
114
115
116
117
118
119
120
121
122
123
124
125
126

Bulk samples of 9 carbonaceous chondrites, comprising of the CI chondrite Orgueil, three CM chondrites (Cold Bokkeveld, Murray and Murchison), two CO chondrites (Ornans and Lance) and three CV3 chondrites (Allende, Grosnaja and Mokoja) were analysed to investigate their Te stable isotope fractionation. Additionally, two EH4 enstatite chondrites (Indarch and Abee) and six ordinary chondrites were measured: three LL chondrites (Bishunpur, LL3.1, Parnallee, LL3.6 and Tuxtuac, LL5), the L3.7 chondrite Mezö-Madaras and two H chondrites (Dhajala, H3.8 and Kernouve H6). For this study meteorite falls were exclusively studied to minimize the impact of terrestrial weathering.

Tellurium analyses of most terrestrial samples are more challenging compared to measurements of chondrites (Te contents of bulk chondrites: ~0.5-2.5 ppm, e.g. Fehr et al., 2005) due to their generally low Te concentrations. Most terrestrial crustal and mantle samples contain only a few ppb Te (e.g. Hein et al., 2003; Terashima, 2001). Eight terrestrial samples with known Te contents of 0.1 - 31 ppm Te (Table 1) were chosen in order to test our new analytical methodologies for a variety of sample matrixes and to start developing a framework for terrestrial Te stable isotope data. Additionally, the Te content and isotope composition of the USGS reference sample SDO-1 (Devonian Ohio shale) was determined. Six of the investigated terrestrial samples are sediments, including two manganese nodules, Nod-P-1 (Pacific ocean) and Nod-A-1 (Atlantic ocean), green river shale SGR-1 (Utah), marine mud Mag-1 (Gulf of Maine, Atlantic) and stream sediment JSD-2. A further three USGS geochemical exploration reference samples were also investigated: Jasperoid GXR-1 (Drum mountains, Utah), soil sample GXR-2 (Park City, Utah) and GXR-4 that is a mill heads sample of a porphyry copper ore from Utah (Allcott and Lakin, 1975).

3. ANALYTICAL METHODS

127 **3.1. Sample preparation**

128

129 Water from an 18.2 MΩ·cm -grade Millipore system and Teflon distilled mineral acids
130 were used for all preparation. Sample powders of bulk chondrites (48 - 311 mg) and all
131 terrestrial samples beside the two manganese nodules were digested in Savillex™ vials at
132 130°C using a series of dissolution steps. After each digestion step, the samples were dried
133 down on a hotplate. First, the samples were dissolved in 5 ml of 29 M HF and 1.3 ml 14 M
134 HNO₃ for 1 - 3 days. They were further digested with aqua regia, followed by subsequent
135 digestion with 4.7 M HNO₃. Finally, the samples were dissolved in 6 M HCl. The two
136 manganese nodules were dissolved using 6 M HCl. For double-spiked samples the ¹²⁵Te-¹²⁸Te
137 double spike (see section 3.3) was either added to the sample powders before sample
138 digestion or after completed digestion in the case where samples were split for analysis of
139 both an un-spiked and spiked sample aliquot. Tellurium was then separated from sample
140 matrixes using an anion-exchange separation procedure optimised after Fehr et al. (2004).
141 Most matrix elements were separated from Te using the “HCl-method” detailed in Fehr et al.
142 (2004) where samples are loaded in 2 M HCl onto 2 ml of AG1-X8 resin (200-400 mesh).
143 The Te fractions were further purified using additional two separation steps using 1 ml and
144 0.2 ml of AG1-X8 resin. The purity of the final Te fractions was checked and tests using
145 synthetic solutions were performed to ensure that any residual matrix elements present did not
146 impact on the accuracy of the Te isotope data (Fehr et al., 2004, 2006, 2009). Yields of the
147 total procedure are approximately 55 %. Total procedural blanks are ≤ 11 pg Te and are
148 insignificant given that processed sample aliquots contain at least 26 ng Te.

149

150 **3.2. Te isotope analyses**

151

152 Tellurium isotope measurements were obtained with a Neptune multiple-collector
153 inductively coupled plasma mass spectrometer (MC-ICPMS) housed at the Open University.
154 Samples and standards were dissolved in 3% HNO₃ and introduced to the mass spectrometer
155 using a PFA nebulizer with either a 20 or 50 μl min⁻¹ flow-rate and an Aridus II desolvation
156 nebulizer system. Normal sampler and X skimmer cones were used for analyses of sample
157 and standard solutions containing 15- 30 ppb Te. Three sample analyses of manganese
158 nodules were performed at 100 ppb Te using both standard sampler and skimmer cones. Ion
159 beams were collected simultaneously on the Faraday cups at the following masses; 125
160 (¹²⁵Te), 126 (¹²⁶Te, ¹²⁶Xe), 128 (¹²⁸Te, ¹²⁸Xe), 129 (¹²⁹Xe), 130 (¹³⁰Te, ¹³⁰Xe, ¹³⁰Ba), and 135
161 (¹³⁵Ba). For both samples and standards we used the following measurement protocol. Before
162 each analysis the system was washed with 3% HNO₃ for 5-10 minutes and on-peak
163 backgrounds were then measured by collecting 40 ratios each with 4.2 s integration time,
164 divided into 2 blocks of analyses. The sample or standard was then measured, with 100 Te
165 isotope ratios collected each with 4.2 s integration time, separated into 5 blocks of analyses.
166 Baselines of Faraday cups were collected with defocused ion beam for 30 s prior to each
167 block of sample and standard measurements and at the start of each background analysis.

168

169 **3.3 Tellurium double-spike procedure**

170

171 To accurately characterise the stable isotope composition of Te, we developed a ¹²⁵Te-
172 ¹²⁸Te double spike methodology. The double spike composition was chosen to minimise
173 analytical uncertainties based on error propagation in the double spike calculations, as well as
174 to minimise interference corrections. Rudge et al. (2009) list a number of Te double spike
175 combinations that are estimated to provide smaller uncertainties (by up to 35 % based on
176 counting statistics) compared to utilising a ¹²⁵Te-¹²⁸Te double spike. However, many of these
177 double-spike combinations use the less abundant Te isotopes that suffer from interferences

178 from Sn (^{120}Te , ^{122}Te , ^{124}Te) and Sb (^{123}Te), whereas the more abundant Te isotopes have
 179 interferences from the rare gas Xe (^{126}Te , ^{128}Te , ^{130}Te) and Ba (^{130}Te), with ^{125}Te being the
 180 only interference free Te isotope. Therefore, we chose to utilize the more abundant Te
 181 isotopes, ^{125}Te to ^{130}Te , which allows for a static data collection and avoids the smaller Te
 182 isotopes that suffer from Sn interferences and therefore minimises analytical uncertainties.
 183 Additionally, the use of a ^{125}Te - ^{128}Te double spike with a $^{125}\text{Te}/^{128}\text{Te}$ ratio of 1.13 provides a
 184 small error magnification in the Te stable isotope determination over a large range of double
 185 spike – sample mixtures (Fig. 1).

186 While sample and standard analyses were background corrected using on-peak
 187 background measurements, small amounts of residual Xe and Ba required interference
 188 corrections for these elements and were performed using the measured abundance of ^{129}Xe
 189 and ^{135}Ba . Results are expressed as $\delta^{130}\text{Te}/^{125}\text{Te} = [(\frac{^{130}\text{Te}/^{125}\text{Te}_{\text{sample}}}{^{130}\text{Te}/^{125}\text{Te}_{\text{Te Alfa Aesar metal}}}) - 1] \times 1000$ relative to a Te Alfa Aesar metal standard (Fehr et al., 2004). The double
 190 spike equations are solved using an iterative Newton Raphson-procedure assuming an
 191 exponential mass fractionation law to derive the fractionation factors (f) of the sample (nat)
 192 and double spike – sample mixture (mix), as well as the proportion (X) of double spike (sp) in
 193 the mixture (e.g. Albarède and Beard, 2004; Bonnand et al., 2011):

$$F^i(X_{sp}^{ref}, f_{nat}, f_{mix}) = X_{sp}^{ref} r_{sp}^i + (1 - X_{sp}^{ref}) r_{nat}^i \left(\frac{M^i}{M^{ref}} \right)^{f_{nat}} - r_{mix}^i \left(\frac{M^i}{M^{ref}} \right)^{f_{mix}} = 0$$

195 where r are the isotope ratios of the double spike, sample and mixture and M are the
 196 true masses of the isotopes (i; ^{125}Te , ^{126}Te , ^{128}Te) and the reference isotope ^{130}Te (ref).

197 The long-term reproducibility of the Te Alfa Aesar metal standard (154 analyses over
 198 10 analytical sessions) is 0.064‰ for $\delta^{130/125}\text{Te}$, whereas internal errors (2 SE) of sample
 199 analyses vary from 0.017 to 0.053‰. Internal errors were related to measured signal
 200 intensities that varied with analyte concentrations and daily sensitivity. Errors for samples
 201 quoted in the manuscript and tables are 2 standard deviations (2 SD) of repeat analyses,

202 whereas for individual sample analyses the daily reproducibility of the Te standard is quoted
203 as the uncertainty.

204 The Te concentration of the ^{125}Te - ^{130}Te double spike was determined by inverse-
205 isotope dilution relative to a gravimetrically prepared dilute solution of SRM 3156. Therefore,
206 the Te concentrations in the samples can be determined by isotope dilution as a by-product of
207 the Te isotope analyses.

208

209 **3.4 Accuracy and precision of Te isotope and concentration data**

210

211 The daily reproducibility of standard solutions ranged from 0.04 to 0.12‰ (2 SD) for
212 $\delta^{130/125}\text{Te}$, whereas sample analyses that were typically repeated over several analytical
213 sessions display slightly more variable results with a reproducibility of 0.02 – 0.2‰ (Tables 1
214 and 2). The number of repeat analyses is small though, where only 4 sample aliquots were
215 measured ≥ 4 times. The reproducibility of $\delta^{130/125}\text{Te}$ for different sample dissolutions varies
216 from 0.003 to 0.58‰ and hence indicates to the presence of sample heterogeneities, in
217 particular for Orgueil (2 SD of 0.42‰) and Mezö-Madaras (2 SD of 0.58‰), whereas other
218 samples display reproducibilities of different dissolutions at ≤ 0.26 ‰. For all samples beside
219 Orgueil (4 aliquots) and Allende (3 aliquots), only one or two separate sample aliquots were
220 dissolved though. Analyses of Allende display a reproducibility of 0.17‰ for $\delta^{130/125}\text{Te}$.

221 Chondrite sample aliquots that were spiked before sample digestion display in general
222 slightly lower Te contents by $\sim 10\%$ on average compared to sample aliquots that were spiked
223 before sample digestion (Table 2, footnote e). This may potentially be indicative of Te loss
224 during sample digestion. However, uncertainties of the Te concentration data are estimated to
225 be up to several % reflecting relatively large uncertainties associated with weighing of small
226 aliquots of the Te double spike. Furthermore, Te concentration data from the literature
227 generally agree well with the data obtained in this study (Table 1, 2). Sample aliquots that

228 were spiked after sample digestion display only small differences in general and no
229 systematic difference in the obtained $\delta^{130/125}\text{Te}$ data compared to sample aliquots that were
230 spiked before sample digestion (Table 2). Therefore, the data indicates that both spiking
231 procedures provide accurate Te stable isotope data.

232 The accuracy of the employed methods was tested using three aliquots of the Te Alfa
233 Aesar metal standard. Aliquots of 50 – 300 ng of Te standard were spiked with the ^{125}Te - ^{128}Te
234 double spike and processed using the anion-exchange separation procedure noted in section
235 3.1. Two column processed aliquots of the Te Alfa Aesar metal standard display small
236 positive deviations from the unprocessed standard ($\delta^{130/125}\text{Te} = 0$) with up to $0.11 \pm 0.08 \%$
237 for $\delta^{130/125}\text{Te}$ (Table 1). On average, column processed aliquots of the Te Alfa Aesar metal
238 standard display a $\delta^{130/125}\text{Te}$ of $0.07 \pm 0.10 \%$ that is identical to the unprocessed standard
239 within uncertainty.

240 In bulk meteorite samples, no resolvable nucleosynthetic or radiogenic Te isotope
241 anomalies are present (Fehr et al., 2005). Therefore, only a spiked sample analysis is in
242 principle necessary to determine the Te mass dependent fractionation of samples. However, it
243 is possible that small, so-far unresolvable, nucleosynthetic Te isotope variations exist. The
244 effect of such potential anomalies on the obtained $\delta^{130/125}\text{Te}$ results is investigated by varying
245 the natural composition of the Te standard that is used in the deconvolution of the double
246 spike equations based on the measured Te isotope variations for bulk chondrites of Fehr et al.
247 (2005). These so far unresolvable potential nucleosynthetic Te isotope variations could
248 produce a maximum variation of 0.27 ‰ in the measured $\delta^{130/125}\text{Te}$. Further analyses were
249 performed in this study on a few selected un-spiked chondrite sample aliquots to verify the
250 inexistence of nucleosynthetic and radiogenic Te isotope anomalies. These new data also
251 indicate that the impact of nucleosynthetic anomalies onto the $\delta^{130/125}\text{Te}$ results is $\leq 0.2 \%$.

252 The accuracy of terrestrial sample analyses was tested by analyses of un-spiked
253 terrestrial sample aliquots, which have identical Te isotope compositions as standard solutions
254 within analytical uncertainty.

255

256 **4. RESULTS**

257 **4.1. Tellurium concentration data**

258

259 Tellurium concentration data were obtained by isotope-dilution as part of the Te stable
260 isotope analyses. For all samples beside SDO-1, literature Te concentration data are available
261 and in general agree well with the data obtained in this study (Table 1, 2). The analysis of
262 USGS reference sample SDO-1 gives a Te content of 0.12 ppm (Table 1) and hence SDO-1
263 has a similar Te content as the green river shale SGR-1 (0.2 ppm) and the marine mud rock
264 Mag-1 (0.05-0.07 ppm).

265

266 **4.2. Tellurium stable isotope results of terrestrial samples**

267

268 The nine terrestrial samples analysed in this study show a range of 0.89‰ for
269 $\delta^{130/125}\text{Te}$ (0.18‰ amu^{-1} , Table 1, Figs. 2 and 3b) with values ranging from -0.15 ± 0.07
270 (GXR-2) to 0.74 ± 0.05 (Nod-A-1). The sediment and USGS geochemical exploration
271 samples studied here cover a similar range in their Te stable isotope composition, beside
272 Nod-A-1 that displays a slightly more positive $\delta^{130/125}\text{Te}$ of 0.74 ± 0.05 ‰.

273

274 **4.3. Tellurium stable isotope results of chondrites**

275

276 The Te stable isotope composition of the investigated chondrites displays an overall
277 variation of 6.3‰ for $\delta^{130/125}\text{Te}$ (1.3‰ amu^{-1} , Table 2, Fig. 1), whereas the unequilibrated

278 ordinary chondrites Mezö-Madaras (L3.7) and Dhajala (H3.8) display the most extreme Te
279 stable isotope signatures with $\delta^{130/125}\text{Te} = -4.12 \pm 0.58$ and 2.15 ± 0.08 , respectively. The Te
280 isotope results obtained in this study for Mezö-Madaras using the double-spike methodology
281 overlaps within uncertainties of previous results ($\delta^{130/125}\text{Te} = -4.72 \pm 2.25$) obtained using a
282 standard-sample bracketing technique (Fehr et al., 2005). There is no correlation of Te isotope
283 fractionation with Te contents or petrographic types of ordinary chondrites (Fig. 4a).
284 Carbonaceous chondrites show a smaller variation in the Te stable isotope composition at
285 0.78‰ for $\delta^{130/125}\text{Te}$ (0.14‰ amu^{-1}), with Orgueil (CI) having the most positive $\delta^{130/125}\text{Te}$
286 signature of 0.36 ± 0.17 for one of the investigated sample splits and an average of $0.04 \pm$
287 0.42‰ for 4 individually digested sample aliquotes. By contrast, Allende (CV3) and Lance
288 (CO3.5) show the most negative $\delta^{130/125}\text{Te}$ values obtained for carbonaceous chondrites with -
289 $0.30 \pm 0.17 \text{‰}$ and $-0.35 \pm 0.20 \text{‰}$ on average, with one sample aliquot of Lance having the
290 most negative $\delta^{130/125}\text{Te}$ of $-0.42 \pm 0.05 \text{‰}$ (Table 2). The enstatite chondrites display a
291 slightly more negative Te isotope signature compared to most carbonaceous chondrites with
292 $\delta^{130/125}\text{Te} = -0.56 \pm 0.07$ for Abee (EH4) and $\delta^{130/125}\text{Te} = -0.35 \pm 0.08$ for Indarch (EH4).

293 In summary, chondritic meteorites display a much wider range of stable Te isotope
294 compositions (6.3‰ for $\delta^{130/125}\text{Te}$) than the small number of terrestrial samples (0.9‰ for
295 $\delta^{130/125}\text{Te}$) studied here. Additionally, both enstatite chondrites and the CV and CO
296 carbonaceous chondrites have more negative $\delta^{130/125}\text{Te}$ compared to the terrestrial samples.

297

298 **5. DISCUSSION**

299

300 **5.1. Tellurium stable isotope fractionation of terrestrial samples**

301

302 Studies investigating Te isotope fractionation using high-precision isotope data of
303 terrestrial samples are so far limited to Te ore minerals, mainly native Te, tellurides and
304 tellurites, where Te isotope variations of 2‰ were observed for $\delta^{130/125}\text{Te}$ (Fornadel et al.,
305 2017; Fornadel et al., 2014). Furthermore, it was suggested that Te isotope fractionation of up
306 to 4‰ in $\delta^{130/125}\text{Te}$ can be generated between different Te ore minerals based on theoretical
307 fractionation models (Fornadel et al., 2017; Smithers and Krouse, 1968). The three
308 geochemical exploration reference samples analysed in this study also display resolvable Te
309 isotope variations of 0.6‰ in $\delta^{130/125}\text{Te}$ (Table 1, Fig. 2). Samples GXR-2 and GXR-4 contain
310 sulfide minerals (Allcott and Lakin, 1975) that are likely the major host phases for Te,
311 whereas sample GXR-1 is a jasperoid.

312 Tellurium distributions have not been studied in detail in sediments, although
313 Schirmer et al. (2014) suggested the Te/Se ratio as a possible paleo-redox proxy. Significant
314 Te isotope fractionation is evident in the terrestrial sedimentary reference samples with a
315 range of 0.85‰ in $\delta^{130/125}\text{Te}$ (Table 1, Fig. 2), highlighting the potential for Te isotopes as a
316 sedimentary geochemical proxy. For many stable isotope systems, redox processes cause
317 some of the largest isotope fractionation (e.g., Beard and Johnson, 2004) and hence might be
318 the cause for some of the observed Te stable isotope variations, consistent with
319 experimentally produced Te isotope fractionation (Baesman et al., 2007; Smithers and
320 Krouse, 1968). The presented data in particular provide the first evidence for significant Te
321 isotope variations in the marine environment based on results for two shales, a mud-rock and
322 two ferromanganese nodules. Ferromanganese crusts and nodules have been used as
323 palaeoceanographic archives that record changes in the composition of seawater through time
324 (e.g., Frank, 2002) and are exceptionally enriched in Te (Hein et al., 2003). As tetravalent and
325 hexavalent Te species can both exist in seawater (Lee and Edmond, 1985), Te isotopes can
326 therefore potentially be used as an oceanographic redox proxy. Estimates of the residence
327 time of Te in the ocean have large uncertainties since information on Te contents of distinct

328 Te sources are sparse. However, it was suggested that Te is likely to have a very short
329 residence time in the ocean of around 100 years (Hein et al., 2003) and hence it is conceivable
330 that ferromanganese crusts and nodules reflect the local seawater composition of Te.
331 Therefore, our new Te isotope data for ferromanganese nodules may suggest the presence of
332 variations in the Te isotope composition of inputs to the ocean. On the other hand, isotope
333 fractionation upon incorporation of Te into ferromanganese crusts and nodules may occur, as
334 has been shown for Mo and Tl (Barling et al., 2001; Rehkämper et al., 2002). Further studies
335 will be necessary to investigate the cause for the observed Te isotope variations in sediments.

336

337 **5.2. Tellurium stable isotope variations in chondrites**

338

339 Tellurium as a moderately volatile element is depleted in different carbonaceous
340 chondrite groups compared to CI chondrites (e.g. Larimer and Anders, 1967), whereas
341 ordinary chondrites are further depleted in moderately volatile elements compared to
342 carbonaceous chondrites (e.g. Kallemeyn et al., 1989). The origin of these depletions is
343 generally considered to reflect nebular (e.g. Larimer and Anders, 1967; Palme et al., 1988)
344 and potentially parent-body processes (e.g. Wombacher et al., 2008) and the new Te stable
345 isotope fractionation data are used to inform the different proposed formation scenarios.

346 Shock heating has been suggested to potentially contribute toward the loss of
347 moderately volatile elements (Friedrich et al., 2004) and isotope fractionation in ordinary
348 chondrites. The ordinary and carbonaceous chondrites investigated here are generally only
349 mildly shocked. Our data indicate that shock-grades of up to 3 induce only minimal Te
350 isotope fractionation, since Grosnaja (S3) has a $\delta^{130/125}\text{Te}$ within analytical uncertainty of two
351 CV3 carbonaceous chondrites that show no evidence for shock (S1). Further investigations
352 will be necessary to investigate the effect of higher shock-grades on the Te stable isotope
353 fractionation. Abee is the only sample that might have experienced slightly higher shock at

354 stage S2-4. Since vapor phases are generally enriched in the light isotopes compared to solid
355 phases (e.g., Richter et al., 2002), as has also been suggested by theoretical calculations for Te
356 (Fornadel et al., 2017; Smithers and Krouse, 1968), loss of Te due to strong shock heating
357 could potentially have induced a positive shift of $\delta^{130/125}\text{Te}$ in the shocked meteorite. All
358 beside one of the investigated chondrites (Mezö-Madaras, L3.7) display more positive
359 $\delta^{130/125}\text{Te}$ values compared to Abee and hence the Te stable isotope composition of Abee is
360 likely also unaffected by shock.

361

362 **5.2.1. Tellurium stable isotope variations of carbonaceous and enstatite chondrites**

363

364 *5.2.1.1. Tellurium stable isotope fractionation of Orgueil*

365 Individually dissolved sample aliquots of ~50 mg of Orgueil were investigated in this
366 study, whereas Orgueil displays heterogeneities in trace element abundances for sample sizes
367 of <200 mg (Barrat et al., 2012). However, concentrations of Te varied only slightly from
368 2.18 to 2.31 ppm for the four analysed sample aliquots of Orgueil (Table 2) and display no
369 correlation with the $\delta^{130/125}\text{Te}$ data. Tellurium is a chalcophile element that also displays
370 siderophile behavior and hence there are indications from sequential leach experiments and
371 analyses of different components of carbonaceous chondrites (Fehr et al., 2006; Kadlag and
372 Becker, 2016b) that the major host phases of Te in carbonaceous chondrites are sulfides and
373 metal. Heating experiments also suggest that Te is present in two phases within carbonaceous
374 chondrites (Matza and Lipschutz, 1977). Since virtually no metal is present in Orgueil, Te is
375 likely associated mainly with the sulfide mineral pyrrhotite (Bullock et al., 2005), although
376 small abundances of cubanite (CuFe_2S_3 ; Kerridge et al., 1979), another potential sulfide host
377 phase of Te, have also been reported. In contrast to other CI chondrites, Orgueil only contains
378 pyrrhotite, but not pentlandite. Orgueil experienced a high degree of secondary alteration
379 during which primary pentlandite is thought to be completely replaced by pyrrhotite (Bullock

380 et al., 2005). There are also indications that sulfate may be another significant Te-bearing
381 phase within Orgueil based on Te contents of hot water leaches (Reed and Allen, 1966; Fehr
382 et al., 2006). The majority of sulfate in Orgueil is considered to have formed during terrestrial
383 sample storage (Gounelle and Zolensky, 2001) from primary sulfate and/or oxidation of
384 sulfides (Gounelle and Zolensky, 2001; Kerridge et al., 1979). Furthermore, sulfur-bearing
385 organic phases are present in carbonaceous chondrites (Gao and Thiemens, 1993a). Therefore,
386 part of the chalcophile element Te may also be associated with organics in Orgueil. The
387 differences in the Te stable isotope composition of different sample fractions of Orgueil
388 (Table 2, Fig. 3) suggest the presence of phases with distinct $\delta^{130/125}\text{Te}$ that are
389 heterogeneously distributed in Orgueil. Pyrrhotite, cubanite, pentlandite, sulphate and organic
390 phases as potential Te host phases in Orgueil may display distinct Te stable isotope signatures
391 and hence the observed Te stable isotope variations of different sample aliquots of Orgueil
392 could be explained by heterogeneously distributed Te-bearing minerals. In contrast, different
393 sample splits of Allende display smaller variations in their Te isotope composition, suggesting
394 that aqueous alteration may be potentially responsible for the heterogeneity of the Te stable
395 isotope compositions in Orgueil. Alternatively, Te might get redistributed by metamorphism,
396 which could have affected in particular CO3 and CV3 carbonaceous chondrites and hence
397 Allende. However, further investigations will be necessary to determine whether sample
398 heterogeneity in terms of Te stable isotope variations increase with degree of aqueous
399 alteration and lower metamorphic grade in carbonaceous chondrites, or whether Te stable
400 isotope composition and Te contents of different Te host phases of Orgueil and other
401 chondrite samples affect the observed Te stable isotope variations.

402

403 *5.2.1.2. Depletion of moderately volatile elements*

404 The concentrations of moderately and highly volatile elements decreases in
405 carbonaceous chondrites from CI to CM, CO and to CV chondrites (e.g., Palme et al., 1988).

406 This depletion is thought to reflect incomplete condensation in hot areas of the nebula, where
407 more volatile elements condensed only partly due to their lower condensation temperature
408 compared to more refractory elements (e.g., Palme et al., 1988). Chondrites are a mixture of
409 chondrules, which experienced melting and are generally depleted in volatile elements and
410 matrix that consists of material that experienced less processing in the nebula and is enriched
411 in volatile elements (e.g. Zanda, 2004; Jones et al., 2005). Tellurium is also depleted in the
412 chondrules of Allende and Murchison compared to matrix fractions (Kadlag and Becker,
413 2016b). The abundance of chondrules increases with higher depletion of Te and other
414 moderately volatile elements in carbonaceous chondrites (Kadlag and Becker, 2016b; Krot et
415 al., 2003). Hence, chondrule formation may be responsible for the depletion of moderately
416 volatile elements in different carbonaceous chondrites groups compared to CI chondrites (e.g.,
417 Alexander et al., 2001). The mass dependent Te isotope composition displays a general
418 correlation with the Te content in carbonaceous chondrites (Fig. 4b), with one aliquot of the
419 CI chondrite Orgueil displaying the most positive $\delta^{130/125}\text{Te}$ signature, whereas three
420 additional Orgueil sample splits have a Te stable isotope composition close to 0. Isotopically
421 light Te is expected to be enriched in volatile components (Fornadel et al., 2017; Smithers and
422 Krouse, 1968). Therefore, Te depletions due to volatile loss or incomplete condensation of Te
423 would generally be expected to produce positive $\delta^{130/125}\text{Te}$ values in different carbonaceous
424 chondrite groups compared to CI. Hence, the observed Te stable isotope fractionation is
425 unlikely caused by the process that is responsible for the depletion of Te. Similar correlations
426 of moderately volatile element depletion with stable isotope variations of Zn and Cu were
427 reported and associated with compositional differences within carbonaceous chondrites due to
428 mixtures of two meteorite components (Luck et al., 2005), as will be further discussed in the
429 next section.

430

431 *5.2.1.3. Oxidation state and variations in the solar nebula*

432 Sulfide phases are expected to be important carriers of Te in chondrites (Allen and
433 Mason, 1973; Fehr et al., 2006; Kadlag and Becker, 2016a). However, empirical and
434 theoretical data for Te isotope fractionation in sulfide phases are not available. In magmatic
435 terrestrial systems, Te is highly incompatible in monosulfide solutions and may exist as Te (0)
436 in sulfides (Helmy et al., 2010). Tellurium is expected to be chalcophile in Orgueil (as no
437 metal is present) and have both siderophile and chalcophile tendencies in carbonaceous
438 chondrites (Fehr et al., 2006; Kadlag and Becker, 2016b), whereas Te is mainly siderophile in
439 enstatite chondrites (Kadlag and Becker, 2015). Hence, Te behaves in an increasingly
440 siderophile manner with decreasing oxidation states of chondrites, whereas enstatite
441 chondrites are more reduced compared to the carbonaceous chondrites. Hence, the overall
442 trends of mass dependent Te isotope composition displays a general trend with the oxidation
443 state of carbonaceous and enstatite chondrites. Ordinary chondrites that are intermediate in
444 oxidation state between carbonaceous and enstatite chondrites display a large spread in Te
445 stable isotope variations, as will be discussed in the following section (5.2.2). On average,
446 ordinary chondrites have a Te stable isotope composition that is intermediate between
447 carbonaceous and enstatite chondrites with -0.4 ± 4.1 in $\delta^{130/125}\text{Te}$ and also fit into the trend of
448 Te stable isotope composition versus oxidation state. Isotopically heavy Te is generally
449 expected to be enriched in more oxidized mineral phases (Fornadel et al., 2017) and could
450 therefore explain the observed difference between enstatite and carbonaceous chondrites. This
451 could also explain the small differences between different groups of carbonaceous chondrites
452 and the most positive $\delta^{130/125}\text{Te}$ values for the most oxidized sample Orgueil. However,
453 aqueous alteration and parent body metamorphism might also have affected the Te stable
454 isotope signature of carbonaceous chondrites. Nevertheless, the observed differences in the Te
455 stable isotope composition of different carbonaceous and enstatite chondrite groups might be
456 a nebular signature that reflects different redox environments within the early solar system.

457 Different chondrite groups and different carbonaceous chondrite classes display
458 distinct nucleosynthetic isotope anomalies for several refractory elements, such as Cr, Zr and
459 Mo, providing evidence for mixtures of two or more components in the early solar system
460 (e.g., Dauphas et al., 2002; Trinquier et al., 2007; Burkhardt et al., 2011; Akram et al., 2015).
461 Different groups of chondrites display different oxidation states and are expected to have
462 formed in different regions of the solar nebula (e.g. Brearley and Jones, 1998) and potentially
463 at different heliocentric distances (e.g. Rubie et al., 2015), as is also reflected in, for example,
464 their Ru mass-independent isotope signature (Fischer-Gödde et al., 2017). Compositional
465 variations of refractory elements and volatile elements might be linked as is evident by
466 correlations of Cr with O mass-independent isotope variations (Trinquier et al., 2007).
467 Additionally, variations in the Cu and Zn isotope stable isotope fractionation also display a
468 correlation with mass-independent O isotope variations in carbonaceous chondrites (Luck et
469 al., 2005). Luck et al. (2005) suggested that these Cu and Zn isotope variations reflect
470 mixtures of two meteorite components within carbonaceous chondrites. According to Luck et
471 al. (2005), one of these components could be represented by refractory inclusions that would
472 be depleted in moderately volatile elements and enriched in the light isotopes due to reaction
473 with an isotopically light gas phase. Tellurium is similar to other moderately volatile elements
474 and is generally depleted in refractory inclusions compared to bulk samples (Brennecka et al.,
475 2016; Fehr et al., 2009). The available Te isotope fractionation data for refractory inclusions
476 from Allende though have large uncertainties at $>10\%$ for $\delta^{130/125}\text{Te}$ and display no resolvable
477 fractionation (Fehr et al., 2009). Hence, further work will be necessary to determine the origin
478 of the small Te stable isotope variations of different chondrites groups to identify meteorite
479 components with distinct compositions. Such a model would also be valid if small so far
480 unresolved nucleosynthetic Te isotope variations would contribute to the differences in
481 $\delta^{130/125}\text{Te}$ ($\leq 0.27\%$; section 3.4). Sulfur and Se are both chalcophile and moderately volatile
482 elements that are geochemically akin to Te. Importantly, S displays also small compositional

483 differences in its mass dependent isotope composition for different chondrite groups (Gao and
484 Thiemens, 1993b), whereas Se displays no systematic variations with present analytical
485 uncertainties of around 0.1 ‰/amu (Vollstaedt et al., 2016). While further investigations
486 combining high precision Te isotope analyses of spiked and unspiked sample aliquots will be
487 necessary to verify how much nucleosynthetic variation exists, our data indicate that there are
488 only small variations in the Te mass dependent stable isotope composition of carbonaceous
489 chondrites.

490

491 **5.2.2. Tellurium stable isotope variations in ordinary chondrites**

492

493 Unequilibrated ordinary chondrites are the least modified meteorites, which contrasts
494 with other chondrite groups whose composition is modified by metamorphism and aqueous
495 alteration. Unequilibrated ordinary chondrites display larger Te stable isotope fractionation
496 compared to ordinary chondrites of higher metamorphic grades with both positive and
497 negative fractionation compared to most chondrites (Table 2, Fig. 3, Fig. 4). These large
498 variations are not only manifested in Mezö-Madaras (L3.7) and Dhajala (H3.8), which display
499 the most extreme Te stable isotope results. Parnallee (LL3.6) and Bishunpur (LL3.1) also
500 display a spread of 0.87‰ in $\delta^{130/125}\text{Te}$, whereas Tuxtuac (LL5) and Kernouve (H6) have
501 $\delta^{130/125}\text{Te}$ values that overlap with the Te isotope composition of CV chondrites. The
502 unequilibrated and equilibrated ordinary chondrites analysed in this study display very similar
503 depletions of Te with an average of 0.28 ± 0.12 and 0.31 ± 0.03 ppm (Table 2), respectively.
504 Similar systematics in isotope fractionation are also observed for the highly volatile element
505 Cd (Wombacher et al., 2008). In contrast, Zn displays more isotope variability in equilibrated
506 ordinary chondrites (Luck et al., 2005). It is conceivable that primitive isotope signatures
507 were retained in unequilibrated ordinary chondrites and were erased by homogenization and
508 redistribution of Te during secondary processes such as metamorphism and aqueous alteration

509 in other chondrite groups. Tellurium is expected to condense into the metal phase and
510 possibly into troilite during condensation from gas of solar composition (Lodders, 2003).
511 Hence, metal is an important host phase for the chalcophile element Te in addition to sulfides,
512 as is supported by geochemical analyses of different ordinary chondrite components (Allen
513 and Mason, 1973; Kadlag and Becker, 2016a; Mason and Graham, 1970). Tellurium seems to
514 display variable behaviour in different unequilibrated ordinary chondrites with primarily
515 siderophile behaviour in three investigated samples including Parnallee (Kadlag and Becker,
516 2016a; Kadlag and Becker, 2017) and predominantly chalcophile behaviour in one sample.
517 The majority of primary metal and sulfide phases are expected to have been modified during
518 chondrule formation and metamorphism (e.g., Scott and Krot, 2014) and therefore the Te
519 stable isotope variations of ordinary chondrites is unlikely to be an undisturbed primary
520 nebular signature.

521

522 *5.2.2.1. Chondrule formation*

523 Tellurium and other moderately volatile elements are depleted in chondrules relative
524 to matrix (Bland et al., 2005; Kadlag and Becker, 2016a) and hence chondrule formation may
525 be an important process that depleted those elements in chondrites and in particular in
526 ordinary chondrites with their high abundance of chondrules (e.g., Larimer and Anders,
527 1967). Chondrules display no resolvable isotope fractionation for other moderately volatile
528 elements including K (Alexander et al., 2000). In contrast, chondrules of unequilibrated
529 ordinary chondrites display isotope fractionation of 2 – 3 ‰/amu for the highly volatile
530 element Cd (Wombacher et al., 2008). Matrix, chondrules and bulk samples however, display
531 very similar amounts of Cd isotope fractionation, indicating that the isotope signature of
532 chondrules and matrix was produced in the same environment. Therefore, the observed
533 isotope fractionation for Te and other moderately and highly volatile elements in ordinary

534 chondrites is not likely to be produced by chondrule formation. Further studies investigating
535 Te isotope fractionation in chondritic components are necessary to verify this conclusion.

536

537 *5.2.2.2. Parent-body metamorphism*

538 Metal and sulfides that are likely the main carrier phases of Te in ordinary chondrites
539 (Kadlag and Becker, 2016a; Mason and Graham, 1970) are probably redistributed during
540 parent-body metamorphism (Grossman and Brearley, 2005; Zanda et al., 1994). It has been
541 suggested that the depletion of moderately and highly volatile elements in ordinary chondrites
542 is caused by parent body processes, where elements may be mobilised during metamorphism
543 (e.g., Schaefer and Fegley Jr., 2010). Tellurium is not systematically depleted in higher
544 metamorphic grade ordinary chondrites though compared to ordinary chondrites of lower
545 metamorphic grades (Kallemeyn et al., 1989; Wolf and Lipschutz, 1998), as is also supported
546 from the data obtained in this study (Table 2, Fig. 4a). There are indications though that Te
547 concentrations in ordinary chondrites are more variable compared to the moderately volatile
548 elements Se and Zn (Schaefer and Fegley Jr., 2010) for example. Tellurium stable isotope
549 fractionation data of ordinary chondrites display no trend with Te concentrations (Fig. 4a),
550 whereas Te contents vary considerably in the investigated samples from 0.19 to 0.35 ppm
551 (Table 2).

552 Heating experiments indicate that a large proportion of the Te budget of ordinary
553 chondrites is lost at temperatures of 873 K and more (Ikramuddin et al., 1977), whereas there
554 is also evidence for a Te phase that releases Te at lower temperatures (673 K; Laurretta et al.,
555 2002). Furthermore, theoretical calculations predict that half of the Te budget gets mobilised
556 at 572 K (at 10^{-4} bar) – 757 K (at 1 bar) during metamorphism (T_m : 50% metamorphic
557 temperature) of ordinary chondrites (Schaefer and Fegley Jr., 2010), whereas the 50%
558 condensation temperature of Te is 709 K (Lodders, 2003). Particularly important is the
559 thermal stability of the Te host-phases as was indicated by the distribution of Zn and Se and

560 their isotope fractionation in ordinary chondrites (Vollstaedt et al., 2016). Hence, given that
561 metamorphic temperatures in unequilibrated ordinary chondrites are estimated to range from
562 around 473 K to up to 873-973 K (e.g., Huss et al., 2006), Te is expected to be mobilised
563 during metamorphism on the ordinary chondrite parent bodies and some Te may also have
564 been lost or redistributed even from unequilibrated ordinary chondrites. In contrast, in some
565 unequilibrated ordinary chondrite components, Te displays correlations with the siderophile
566 refractory element Ir and with Pd, which may suggest that Te was not affected by
567 metamorphism (Kadlag and Becker, 2017). Hence, this may indicate that the Te stable isotope
568 signatures in unequilibrated chondrites might be a primary nebula signature or produced by
569 chondrule formation. However, sulphide and metal phases are often inter-grown in chondrites
570 and consist of multiple primary and secondary phases (e.g. Brearley and Jones, 1998; Scott
571 and Krot, 2014), which complicates the interpretation of element abundance patterns of
572 chondrite components.

573 Highly volatile and some moderately volatile elements including Ag, Cd, Rb and Zn
574 display isotope fractionation in ordinary chondrites thought to be produced by metamorphic
575 parent-body processes (Luck et al., 2005; Nebel et al., 2011; Schönbächler et al., 2008;
576 Wombacher et al., 2008; Wombacher et al., 2003). The present study confirms that stable
577 isotope fractionation is also evident for Te in unequilibrated ordinary chondrites, as was
578 initially suggested by Fehr et al. (2005). Tellurium ($T_m = 572$ K; $T_c = 709$ K) displays slightly
579 more isotope variations overall with 1.3‰ amu^{-1} compared to the moderately volatile
580 elements Zn ($T_m = 840$ K; $T_c = 726$ K;), Ag ($T_m = 875$ K; $T_c = 996$ K) and Rb ($T_m = 675$ K; T_c
581 $= 800$ K) that have slightly higher 50% metamorphic and condensation temperatures at 10^{-4}
582 bar (Lodders, 2003; Schaefer and Fegley Jr., 2010) and display $0.5 - 0.7 \text{‰ amu}^{-1}$
583 fractionation (Luck et al., 2005; Nebel et al., 2011; Schönbächler et al., 2008). Selenium has a
584 condensation temperature of 697 K (Lodders, 2003) and a slightly higher 50% metamorphic
585 temperature of 626 K compared to Te at 10^{-4} bar (Schaefer and Fegley Jr., 2010) but displays

586 no resolvable isotope fractionation ($<0.2\text{‰ amu}^{-1}$; Vollstaedt et al., 2016). At 1 bar, Te ($T_m =$
587 757) is estimated to be significantly more mobile during metamorphism compared to Se ($T_m =$
588 875 K; Schaefer and Fegley Jr., 2010). Furthermore, ordinary chondrites display non-
589 significant isotope variability for the moderately volatile element S (Gao and Thiemens,
590 1993b), which is estimated to be less mobile compared to Te during metamorphism (Schaefer
591 and Fegley Jr., 2010). In contrast, larger isotope variations are reported for the highly volatile
592 element Cd ($T_m = 547$ K; $T_c = 652$ K; Lodders, 2003; Schaefer and Fegley Jr., 2010) at 5.8‰
593 amu^{-1} (Wombacher et al., 2008).

594 This non-systematic relationship of isotope fractionation versus depletion in
595 concentration and metamorphic grade can be explained by multiple-stage evaporation and re-
596 condensation of moderately to highly volatile elements in colder parts of the ordinary
597 chondrite parent bodies (Schönbächler et al., 2008; Wombacher et al., 2008). In an onion-
598 shell model, the colder outer part of the parent bodies are considered highly porous
599 facilitating loss of volatile elements as well as re-condensation, whereas the hotter inner
600 regions are regarded as less porous allowing for higher degrees of back-reactions of volatiles
601 (Schönbächler et al., 2008; Wombacher et al., 2008). Importantly, such a model can explain
602 both positive and negative isotope fractionation, as is evident for Te (Fig. 3a). Open-system
603 metamorphism associated with higher porosity and lower internal pressure would require
604 lower temperatures for Te mobilisation compared to closed-system metamorphism (Schaefer
605 and Fegley Jr., 2010). Hence, it is likely that the stable isotope fractionation of Te and other
606 moderately and volatile elements in ordinary chondrites is caused by evaporation and
607 condensation processes during metamorphism on the meteorite parent body. However, further
608 work will be necessary to verify this conclusion and exclude chondrule formation and nebular
609 processes as potential origin for the observed Te stable isotope variations.

610

611 **5.3. The composition of the Earth and the late veneer**

612

613 The solar system is relatively homogeneous in terms of elemental and isotopic
614 compositions, although small variations between different planets and meteorite parent bodies
615 exist (Palme et al., 2014). These small compositional differences provide important
616 information on the building blocks of the Earth, which in the past were considered to have a
617 similar chemical and isotopic composition to chondritic meteorites. Enstatite chondrites
618 provide a match to the Earth in terms of nucleosynthetic isotopic composition for a number of
619 elements (e.g., Dauphas and Schauble, 2016), whereas in terms of bulk elemental abundances,
620 the composition is closer to carbonaceous chondrites (Palme and O' Neill, 2014). The initial
621 accreting material to the Earth may have been more reduced and later accretion may have
622 involved more oxidized and volatile rich material from the outer solar system (e.g. Wood et
623 al., 2006; Schönbächler et al., 2010). This oxidized, carbonaceous chondrite like material is
624 also expected to have delivered a large part of the moderately volatile element budget to the
625 Earth (Schönbächler et al., 2010). There are also indications, for example, from
626 nucleosynthetic isotope variations of Mo and Ru in chondrites that chondrites cannot have
627 been the main constituents of the Earth (Dauphas et al., 2002; Burkhardt et al., 2011; Fischer-
628 Götde and Kleine, 2017). Therefore, it is conceivable that the building blocks of the Earth
629 might be missing from our meteorite collection because they were accreted during terrestrial
630 planet formation (Dauphas and Schauble, 2016), although material with near-chondritic
631 composition could still make up large parts of the Earth (e.g. Dauphas, 2017).

632 Core formation has depleted the silicate portion of the Earth of siderophile elements.
633 However, the concentrations of highly siderophile elements, as well as the moderately volatile
634 elements Te and Se in the silicate Earth are higher than expected based on partition
635 coefficients and it was suggested that a large portion of these elements was added after core
636 formation by a late veneer (e.g., Kimura et al., 1974; Rose-Weston et al., 2009; Wang and

637 Becker, 2013). Based on Se/Te ratios, Wang and Becker (2013) concluded that the late veneer
638 had a composition similar to CI or CM carbonaceous chondrites. However, near-chondritic
639 Se/Te ratios of Earth's mantle may not be a primary signature, as was suggested by König et
640 al. (2014).

641 The new Te stable isotope data presented here demonstrate that different chondrite
642 groups display differences in their $\delta^{130/125}\text{Te}$ isotope composition. In order to use Te stable
643 isotope fractionation data to deduce information regarding the building blocks of the Earth
644 and the composition of the late veneer, one would need to also know the Te isotope
645 composition of the silicate Earth. The silicate Earth has two orders of magnitude lower Te
646 contents compared to meteorites (e.g., McDonough and Sun, 1995) and hence such analyses
647 are analytically challenging and would require further improvement of the methodologies
648 described here. Further studies will be necessary to investigate the Te stable isotope
649 composition of the silicate Earth. However, assuming that only small stable isotope
650 fractionation is produced on Earth the available Te stable isotope fractionation data for
651 terrestrial samples and standards may provide an estimate for the Te composition of the
652 silicate Earth. The terrestrial samples and standards have a Te stable isotope composition
653 ranging from -0.15 ± 0.07 to $+0.74 \pm 0.05$ for $\delta^{130/125}\text{Te}$ (Table 1). In detail the shales may
654 provide a useful guide to the composition of the silicate Earth as they potentially represent an
655 average crustal composition derived by weathering and they display a slightly narrower range
656 in $\delta^{130/125}\text{Te}$ with -0.08 ± 0.08 and 0.42 ± 0.01 , which overlaps with compositions determined
657 for the CM and CI carbonaceous chondrites (Table 1, 2, Fig. 3b). By contrast, significantly
658 more negative Te isotope compositions of -0.55 ± 0.07 to -0.24 ± 0.08 were determined for
659 the studied CV and enstatite chondrites. The CO carbonaceous chondrite Lance ($\delta^{130/125}\text{Te} = -$
660 0.35 ± 0.20) also displays a more negative Te isotope signature compared to the terrestrial
661 samples, whereas the Te isotope data for the CO chondrite Ornans ($\delta^{130/125}\text{Te} = -0.18 \pm 0.26$)
662 overlaps with the compositional range determined for terrestrial samples. Ordinary chondrites

663 display a large range in Te stable isotope fractionation, although their average composition
664 overlaps though with that of terrestrial samples ($\delta^{130/125}\text{Te} = -0.4 \pm 4.1$). Therefore, the
665 presented data are in agreement with Te derived from a late veneer that has a composition
666 similar to that of CI or CM carbonaceous chondrites, a conclusion also reached by Wang and
667 Becker (2013) based on Se/Te and chalcogen/Ir ratios. However, the recent Ru
668 nucleosynthetic isotope study by Fischer-Gödde and Kleine (2017) indicates that the late
669 veneer has a non-chondritic composition that is most similar to enstatite chondrites. Further
670 work will be necessary to improve our understanding of the behavior of Te during core
671 formation to constrain the late veneer contribution to the Te budget of the silicate Earth and to
672 characterize the Te stable isotope signature of the silicate Earth to deduce whether the Ru and
673 Te isotope data provide contradicting evidence to the composition of the late veneer.

674

675 **6. CONCLUSIONS**

676

677 Significant Te stable fractionation is present in terrestrial sediments of 0.85‰ for
678 $\delta^{130/125}\text{Te}$ indicating that Te isotopes have a potential to become a sedimentary geochemical
679 proxy. Geochemical exploration reference samples display 0.6 ‰ variations in $\delta^{130/125}\text{Te}$.

680 Tellurium displays large isotope fractionation in unequilibrated ordinary chondrites
681 with an overall variation of 6.3‰ for $\delta^{130/125}\text{Te}$, similar to some other moderately and highly
682 volatile elements (Luck et al., 2005; Nebel et al., 2011; Schönbacher et al., 2008;
683 Wombacher et al., 2008; Wombacher et al., 2003). The observed Te isotope fractionations in
684 ordinary chondrites is likely caused by evaporation and condensation processes during parent-
685 body metamorphism or alternatively potentially in the nebula or associated with chondrule
686 formation.

687 Smaller compositional variations in the Te stable isotope composition are present
688 between different groups of carbonaceous chondrites and between enstatite and carbonaceous

689 chondrites, indicating the mixing of two or more components with distinct Te isotope
690 compositions reflecting likely Te isotope fractionation in the early solar system. Parent body
691 processes could also have affected the Te stable isotope signature, as is indicated by the
692 sample heterogeneity of Orgueil. Tellurium isotope variations within carbonaceous and
693 enstatite chondrites display a correlation with the oxidation state of samples and hence might
694 provide a nebular record of the environment where the different groups of chondrites formed.

695 The Te stable isotope composition of terrestrial samples is more positive in $\delta^{130/125}\text{Te}$
696 compared to enstatite and CV carbonaceous chondrites. If the silicate Earth has a similar Te
697 isotope signature to the terrestrial samples and standards investigated in this study, then the
698 present data would be in agreement with a late veneer contribution with composition similar
699 to that of CI, CM or potentially CO chondrites. Future work to determine the Te stable isotope
700 signature of the silicate Earth is necessary though to verify this conclusion.

701

702 *Acknowledgements:* We thank the Natural History Museum in London and the Open
703 University (Allende) for providing the samples from their meteorite collections for this study.
704 Laura Schaefer is thanked for insights to predictions based on estimated formation
705 temperatures during metamorphism. Harry Becker and Tetsuya Yokoyama are thanked for
706 their detailed and constructive reviews. Support from the Centre for Earth, Planetary, Space
707 and Astronomical Research (CEPSAR) at the Open University is gratefully acknowledged.

708

709

710

711

712

713

714

715 **REFERENCES**

716

717 Akram W., Schönbacher M., Bisterzo S. and Gallino R. (2015) Zirconium isotope evidence
718 for the heterogeneous distribution of s-process materials in the solar system. *Geochim.*
719 *Cosmochim. Acta* **165**, 484-500.

720 Albarède F. and Beard B. L. (2004) Analytical methods for non-traditional isotopes. In
721 *Geochemistry of Non-Traditional Stable Isotopes* (eds. C. M. Johnson, B. L. Beard
722 and F. Albarède). The Mineralogical Society of America, pp. 113-152.

723 Alexander C. M. O., Boss A. P. and Carlson R. W. (2001) The early evolution of the inner
724 solar system: A meteoritic perspective. *Science* **293**, 64-68.

725 Alexander C. M. O'.D., Grossman J. N., Wang J., Zanda B., Bourot-Denise M. and Hewins
726 R. H. (2000) The lack of potassium isotopic fractionation in Bishunpur chondrules.
727 *Meteorit. Planet. Sci.* **35**, 859-868.

728 Allcott G. H. and Lakin H. W. (1975) The homogeneity of six geochemical exploration
729 reference samples. In *Geochemical exploration 1974* (eds. I. L. Elliott and W. K.
730 Fletcher). Elsevier, pp. 659-682.

731 Allen R. O. J. and Mason B. (1973) Minor and trace elements in some meteoritic minerals.
732 *Geochim. Cosmochim. Acta* **37**, 1435-1456.

733 Anders E., Higuchi H., Ganapathy R. and Morgan J. W. (1976) Chemical fractionations in
734 meteorites - IX. C3 chondrites. *Geochim. Cosmochim. Acta* **40**, 1131-1139.

735 Axelsson M. D., Rodushkin I., Ingri J. and Öhlander B. (2002) Multielemental analysis of
736 Mn-Fe nodules by ICP-MS: optimisation of analytical method. *Analyst* **127**, 76-82.

737 Baesman S. M., Bullen T. D., Dewald J., Zhang D., Curran S., Islam F. S., Beveridge T. J.
738 and Oremland R. S. (2007) Formation of tellurium nanocrystals during anaerobic
739 growth of bacteria that use Te oxyanions as respiratory electron acceptors. *App.*
740 *Environ. Microbiol.* **73**, 2135-2143.

741 Barling J., Arnold G. L. and Anbar A. D. (2001) Natural mass-dependent variations in the
742 isotopic composition of molybdenum. *Earth Planet. Sci. Lett.* **193**, 447-457.

743 Barrat J. A., Zanda B., Moynier F., Bollinger C., Liorzou C. and Bayon G. (2012)
744 Geochemistry of CI chondrites: Major and trace elements, and Cu and Zn isotopes.
745 *Geochim. Cosmochim. Acta* **83**, 79-92.

746 Beard B. L. and Johnson C. M. (2004) Fe isotope variations in the modern and ancient Earth
747 and other planetary bodies. In *Geochemistry of Non-Traditional Stable Isotopes* (eds.
748 C. M. Johnson, B. L. Beard and F. Albarède). The Mineralogical Society of America,
749 pp. 319-357.

750 Binz C. M., Ikramuddin M., Rey P. and Lipschutz M. E. (1976) Trace elements in primitive
751 meteorites—VI. Abundance patterns of thirteen trace elements and interelement
752 relationships in unequilibrated ordinary chondrites. *Geochim. Cosmochim. Acta* **40**,
753 59-71.

754 Bland P. A., Alard O., Benedix G. K., Kearsley A. T., Menzies O. N., Watt L. E. and Rogers
755 N. W. (2005) Volatile fractionation in the early solar system and chondrule/matrix
756 complementarity. *Proc. Nat. Acad. Sci.* **102**, 13755-13760.

757 Bonnand P., Parkinson I. J., James R. H., Karjalainen A.-M. and Fehr M. A. (2011) Accurate
758 and precise determination of stable Cr isotope compositions in carbonates by double
759 spike MC-ICP-MS. *J. Anal. At. Spectrom.* **26**, 528-535.

760 Brearley A. J. and Jones R. H. (1998) Chondritic meteorites. In: *Planetary Materials* (ed. J. J.
761 Papike). The Mineralogical Society of America, Chap. 3, pp. 398.

762 Brennecka G. A., Borg L. E., Romaniello S. J., Souders A. K., Shollenberger Q. R., Marks N.
763 E. and Wadhwa M. (2016) A renewed search for short-lived ¹²⁶Sn in the early Solar
764 System: Hydride generation MC-ICPMS for high sensitivity Te isotopic analysis.
765 *Geochim. Cosmochim. Acta* **201**, 331-344.

766 Bullock E. S., Gounelle M., Lauretta D. S., Grady M. M. and Russell S. S. (2005) Mineralogy
767 and texture of Fe-Ni sulfides in CI1 chondrites: Clues to the extent of aqueous
768 alteration on the CI1 parent body. *Geochim. Cosmochim. Acta* **69**, 2687-2700.

769 Burkhardt C., Kleine T., Oberli F., Pack A., Bourdon B. and Wieler R. (2011) Molybdenum
770 isotope anomalies in meteorites: Constraints on solar nebula evolution and origin of
771 the Earth. *Earth Planet. Sci. Lett.* **312**, 390-400.

772 Dauphas N. (2017) The isotopic nature of the Earth's accreting material through time. *Nature*
773 **541**, 521-524.

774 Dauphas N., Marty B. and Reisberg L. (2002) Molybdenum nucleosynthetic dichotomy
775 revealed in primitive meteorites. *Astrophys. J.* **569**, L139-L142.

776 Dauphas N. and Schauble E. (2016) Mass fractionation laws, mass-independent effects, and
777 isotopic anomalies. *Annu. Rev. Earth Planet. Sci.* **44**, 709-783.

778 Fehr M. A., Rehkämper M. and Halliday A. N. (2004) Application of MC-ICPMS to the
779 precise determination of tellurium isotope compositions in chondrites, iron meteorites
780 and sulfides. *Int. J. Mass Spectrom.* **232**, 83-94.

781 Fehr M. A., Rehkämper M., Halliday A. N., Hattendorf B. and Günther D. (2009) Tellurium
782 isotope compositions of calcium-aluminum-rich inclusions. *Meteorit. Planet. Sci.* **44**,
783 971-984.

784 Fehr M. A., Rehkämper M., Halliday A. N., Schönbächler M., Hattendorf B. and Günther D.
785 (2006) Search for nucleosynthetic and radiogenic tellurium isotope anomalies in
786 carbonaceous chondrites. *Geochim. Cosmochim. Acta* **70**, 3436-3448.

787 Fehr M. A., Rehkämper M., Halliday A. N., Wiechert U., Hattendorf B., Günther D., Ono S.
788 and Rumble III D. (2005) The tellurium isotopic composition of the early solar system
789 - A search for isotope anomalies from the decay of ^{126}Sn , stellar nucleosynthesis, and
790 mass independent fractionations. *Geochim. Cosmochim. Acta* **69**, 5099-5112.

791 Fischer-Gödde M. and Kleine T. (2017) Ruthenium isotopic evidence for an inner Solar
792 System origin of the late veneer. *Nature* **541**, 525-527.

793 Fornadel A. P., Spry P. G., Haghnegahdar M. A., Schauble E. A., Jackson S. E. and Mills S. J.
794 (2017) Stable Te isotope fractionation in tellurium-bearing minerals from precious
795 metal hydrothermal ore deposits. *Geochim. Cosmochim. Acta* **202**, 215-230.

796 Fornadel A. P., Spry P. G., Jackson S. E., Mathur R. D., Chapman J. B. and Girard I. (2014)
797 Methods for the determination of stable Te isotopes of minerals in the system Au-Ag-
798 Te by MC-ICP-MS. *J. Anal. At. Spectrom.* **29**, 623-637.

799 Frank M. (2002) Radiogenic isotopes: Tracers of past ocean circulation and erosional input.
800 *Rev. Geophys.* **40**, 1-38.

801 Friedrich J. M., Bridges J. C., Wang M.-S. and Lipschutz M. E. (2004) Chemical studies of L
802 chondrites. VI. Variations with petrographic type and shock-loading among
803 equilibrated falls. *Geochim. Cosmochim. Acta* **68**, 2889-2904.

804 Friedrich J. M., Wang M.-S. and Lipschutz M. E. (2002) Comparison of the trace element
805 composition of Tagish Lake with other primitive carbonaceous chondrites. *Meteoritics*
806 **37**, 677-686.

807 Gao X. and Thiemens M. H. (1993a) Isotopic composition and concentration of sulfur in
808 carbonaceous chondrites. *Geochim. Cosmochim. Acta* **57**, 3159-3169.

809 Gao X. and Thiemens M. H. (1993b) Variations of the isotopic composition of sulfur in
810 enstatite and ordinary chondrites. *Geochim. Cosmochim. Acta* **57**, 3173-3176.

811 Georg R. B., Halliday A. N., Schauble E. A. and Reynolds B. C. (2007) Silicon in the Earth's
812 core. *Nature* **447**, 1102-1106.

813 Gounelle M. and Zolensky M. E. (2001) A terrestrial origin for sulfate veins in CI1
814 chondrites. *Meteorit. Planet. Sci.* **36**, 1321-1329.

815 Grossman J. N. and Brearley A. J. (2005) The onset of metamorphism in ordinary and
816 carbonaceous chondrites. *Meteorit. Planet. Sci.* **1**, 87-122.

817 Hall G. E. M. and Pelchat J.-C. (1997) Determination of As, Bi, Sb, Se and Te in fifty five
818 reference materials by hydride generation ICP-MS. *Geostand. Newsl.* **21**, 85-91.

819 Hein J. R., Koschinsky A. and Halliday A. N. (2003) Global occurrence of tellurium-rich
820 ferromanganese crusts and a model for the enrichment of tellurium. *Geochim.*
821 *Cosmochim. Acta* **67**, 1117-1127.

822 Helmy H. M., Ballhaus C., Wohlgemuth-Ueberwasser C., Fonseca R. O. C. and Laurenz V.
823 (2010) Partitioning of Se, As, Sb, Te and Bi between monosulfide solid solution and
824 sulfide melt – Application to magmatic sulfide deposits. *Geochim. Cosmochim. Acta*
825 **74**, 6174-6179.

826 Huss G. R., Rubin A. E. and Grossman J. N. (2006) Thermal Metamorphism in Chondrites. In
827 *Meteorites and the Early Solar System II* (eds. D. S. Lauretta and H. Y. McSween Jr.).
828 Univ. of Arizona Press. pp. 567-586.

829 Ikramuddin M., Binz C. M. and Lipschutz M. E. (1977) Thermal metamorphism of primitive
830 meteorites - III. Ten trace elements in Krymka L3 chondrite heated at 400-1000°C.
831 *Geochim. Cosmochim. Acta* **41**, 393-401.

832 Jones R. H., Grossman J. N. and Rubin A. E. (2005) Chemical, mineralogical and isotopic
833 properties of chondrules: Clues to their origin. In: *Chondrites and the Protoplanetary*
834 *Disk* (eds. A. N. Krot, E. R. D. Scott and B. Reipurth) ASP Conference Series, Vol.
835 341, 251-285.

836 Kadlag Y. and Becker H. (2015) Fractionation of highly siderophile and chalcogen elements
837 in components of EH3 chondrites. *Geochim. Cosmochim. Acta* **161**, 166-187.

838 Kadlag Y. and Becker H. (2016a) ^{187}Re - ^{187}Os systematics, highly siderophile element, S-Se-
839 Te abundances in the components of unequilibrated L chondrites. *Geochim.*
840 *Cosmochim. Acta* **172**, 225-246.

841 Kadlag Y. and Becker H. (2016b) Highly siderophile and chalcogen element constraints on
842 the origin of components of the Allende and Murchison meteorites. *Meteorit. Planet.*
843 *Sci.* **51**, 1136-1152.

844 Kadlag Y. and Becker H. (2017) Origin of highly siderophile and chalcophile element
845 fractionations in the components of unequilibrated H and LL chondrites. *Chemie der*
846 *Erde* **77**, 105-119.

847 Kallemeyn G. W., Rubin A. E., Wang D. and Wasson J. T. (1989) Ordinary chondrites: Bulk
848 compositions, classification, lithophile-element fractionations, and composition-
849 petrographic type relationships. *Geochim. Cosmochim. Acta* **53**, 2747-2767.

850 Kallemeyn G. W. and Wasson J. T. (1986) Compositions of enstatite (EH3, EH4,5 and EL6)
851 chondrites: Implications regarding their formation. *Geochim. Cosmochim. Acta* **50**,
852 2153-2164.

853 Keays R. R., Ganapathy R. and Anders E. (1971) Chemical fractionations in meteorites - IV.
854 Abundances of fourteen trace elements in L-chondrites; implications for
855 cosmochemistry. *Geochim. Cosmochim. Acta* **35**, 337-363.

856 Kerridge J. F., MacDougall J. D. and Marti K. (1979) Clues to the origin of sulfide minerals
857 in CI chondrites. *Earth Planet. Sci. Lett.* **43**, 359-367.

858 Kimura K., Lewis R. S. and Anders E. (1974) Distribution of gold and rhenium between
859 nickel-iron and silicate melts: implications for the abundance of siderophile elements
860 on the Earth and Moon. *Geochim. Cosmochim. Acta* **38**, 683-701.

861 König S., Lorand J.-P., Luguet A. and Pearson D. G. (2014) A non-primitive origin of near-
862 chondritic S–Se–Te ratios in mantle peridotites; implications for the Earth’s late
863 accretionary history. *Earth Planet. Sci. Lett.* **385**, 110-121.

864 Krot A. N., Keil K., Goodrich C. A., Scott C. and Weisberg M. K. (2003) Classification of
865 meteorites. In *Treatise on Geochemistry* (eds. H. D. Holland and K. K. Turekian,
866 K.K.), Chap. 1 (ed. A. M. Davis). Elsevier. pp. 83-128.

867 Larimer J. W. and Anders E. (1967) Chemical fractionations in meteorites-II. Abundance
868 patterns and their interpretation. *Geochim. Cosmochim. Acta* **31**, 1239-1270.

869 Laurretta D. S., Klaue B. and Blum J. D. (2002) Thermal analysis of volatile trace elements in
870 carbonaceous and ordinary chondrites. *Lunar Planet. Sci. XXXIII*. Lunar Planet. Inst.,
871 Houston. #1602(abstr.).

872 Lee D. S. and Edmond J. M. (1985) Tellurium species in seawater. *Nature* **313**, 782-785.

873 Lingner D. W., Huston T. J., Hutson M. and Lipschutz M. E. (1987) Chemical studies of H
874 chondrites. I: Mobile trace elements and gas retention ages. *Geochim. Cosmochim.*
875 *Acta* **51**, 727-739.

876 Lodders K. (2003) Solar system abundances and condensation temperatures of the elements.
877 *Astrophys. J.* **591**, 1220-1247.

878 Luck J.-M., Ben Othman D. and Albarède F. (2005) Zn and Cu isotopic variations in
879 chondrites and iron meteorites: Early solar nebula reservoirs and parent-body
880 processes. *Geochim. Cosmochim. Acta* **69**, 5351-5363.

881 Makishima A. and Nakamura E. (2009) Determination of Ge, As, Se and Te in silicate
882 samples using isotope dilution-internal standardisation octopole reaction cell ICP-
883 QMS by normal sample nebulisation. *Geostand. Geoanal. Res.* **33**, 369-384.

884 Mason B. and Graham A. L. (1970) Minor and trace elements in meteoritic materials.
885 *Smithson. Contrib. Earth Sci.* **3**, 1-17.

886 Matza S. and Lipschutz M. E. (1977) Thermal metamorphism of primitive meteorites - VI.
887 Eleven trace elements in Murchison C2 chondrite heated at 400-1000°C. *Lunar*
888 *Planet. Sci. VIII*. Lunar Planet. Inst., Houston. 161-176 (abstr.).

889 McDonough W. F. and Sun S.-S. (1995) The composition of the Earth. *Chem. Geol.* **120**, 223-
890 253.

891 Morgan J. W., Janssens M.-J., Takahashi H., Hertogen J. and Anders E. (1985) H-chondrites:
892 Trace element clues to their origin. *Geochim. Cosmochim. Acta* **49**, 247-259.

893 Moynier F., Fujii T., Telouk P. and Albarède F. (2008) Isotope separation of Te in chemical
894 exchange system with Dicyclohexano-18-crown-ether. *J. Nucl. Sci. Technol.* **6**, 10-14.

895 Nebel O., Mezger K., and van Westrenen W. (2011) Rubidium isotopes in primitive
896 chondrites: Constraints on Earth's volatile element depletion and lead isotope
897 evolution. *Earth Planet. Sci. Lett.* **305**, 309-316.

898 Palme H., Larimer J. W. and Lipschutz M. E. (1988) Moderately volatile elements. In
899 *Meteorites and the Early Solar System* (eds J. F. Kerridge and M. S. Matthews).
900 University of Arizona, Tucson, AZ, pp 436-461.

901 Palme H., Lodders K. and Jones A. (2014) Solar System Abundances of the Elements. In
902 *Treatise on Geochemistry* 2nd Edition (eds. H. D. Holland and K. K. Turekian), Chap.
903 2 (ed. A. M. Davis). Elsevier. pp. 15-36.

904 Palme H. and O' Neill H. St. C. (2014) Cosmochemical Estimates of Mantle Composition. In
905 *Treatise on Geochemistry* 2nd Edition (eds. H. D. Holland and K. K. Turekian), Chap.
906 3 (ed. R. W. Carlson). Elsevier. pp. 1-39.

907 Pogge von Strandmann P. A. E., Elliott T., Marschall H. R., Coath C., Lai Y.-J., Jeffcoate A.
908 B. and Ionov D. A. (2011) Variations of Li and Mg isotope ratios in bulk chondrites
909 and mantle xenoliths. *Geochim. Cosmochim. Acta* **75**, 5247–5268.

910 Poitrasson F., Halliday A. N., Lee D.-C., Levasseur S. and Teutsch N. (2004) Iron isotope
911 differences between Earth, Moon, Mars and Vesta as possible records of contrasted
912 accretion mechanisms. *Earth Planet. Sci. Lett.* **223**, 253-266.

913 Reed G. W. J. and Allen R. O. J. (1966) Halogens in chondrites. *Geochim. Cosmochim. Acta*
914 **30**, 779-800.

915 Rehkämper M., Frank M., Hein J. R., Porcelli D., Halliday A., Ingri J. and Liebetrau V.
916 (2002) Thallium isotope variations in seawater and hydrogenetic, diagenetic, and
917 hydrothermal ferromanganese deposits. *Earth Planet. Sci. Lett.* **197**, 65-81.

918 Richter F. M., Davis A. M., Ebel D. S. and Hashimoto A. (2002) Elemental and isotopic
919 fractionation of Type B calcium-, aluminum-rich inclusions: Experiments, theoretical
920 considerations, and constraints on their thermal evolution. *Geochim. Cosmochim. Acta*
921 **66**, 521-540.

922 Rose-Weston L., Brenan J. M., Fei Y., Secco R. A. and Frost D. J. (2009) Effect of pressure,
923 temperature, and oxygen fugacity on the metal-silicate partitioning of Te, Se, and S:
924 Implications for earth differentiation. *Geochim. Cosmochim. Acta* **73**, 4598-4615.

925 Rouxel O., Ludden J., Carignan J., Marin L. and Fouquet Y. (2002) Natural variations of Se
926 isotopic composition determined by hydride generation multiple collector inductively
927 coupled plasma mass spectrometry. *Geochim. Cosmochim. Acta* **66**, 3191-3199.

928 Rubie D. C., Jacobson S. A., Morbidelli A., O'Brien D. P., Young E. D., de Vries J., Nimmo
929 F., Palme H. and Frost D. J. (2015) Accretion and differentiation of the terrestrial
930 planets with implications for the compositions of early-formed Solar System bodies
931 and accretion of water. *Icarus* **248**, 89-108.

932 Schaefer L. and Fegley Jr. B. (2010) Volatile element chemistry during metamorphism of
933 ordinary chondritic material and some of its implications for the composition of
934 asteroids. *Icarus* **205**, 483-496.

935 Schirmer T., Koschinsky A. and Bau B. (2014) The ratio of tellurium and selenium in
936 geological material as a possible paleo-redox proxy. *Chem. Geol.* **376**, 44-51.

937 Schönbächler M., Carlson R. W., Horan M. F., Mock T. D. and Hauri E. H. (2008) Silver
938 isotope variations in chondrites: Volatile depletion and the initial Pd-107 abundance of
939 the solar system. *Geochim. Cosmochim. Acta* **72**, 5330-5341.

940 Schönbächler M., Carlson R. W., Horan M. F., Mock T. D. and Hauri E. H. (2010)
941 Heterogeneous accretion and the moderately volatile element budget of Earth. *Science*
942 **328**, 884-87.

943 Scott E. R. D. and Krot A. N. (2014) Chondrites and their components. In *Treatise on*
944 *Geochemistry* 2nd Edition (eds. H. D. Holland and K. K. Turekian), Chap. 1 (ed. A.
945 M. Davis). Elsevier. pp. 65-137.

946 Smithers R. M. and Krouse H. R. (1968) Tellurium isotope fractionation study. *Can. J. of*
947 *Chem.* **46**, 583-591.

948 Takahashi H., Janssen M. J., Morgan J. W. and Anders E. (1978) Further studies of trace
949 elements in C3 chondrites. *Geochim. Cosmochim. Acta* **42**, 97-106.

950 Terashima S. (2001) Determination of indium and tellurium in fifty nine geological reference
951 materials by solvent extraction and graphite furnace atomic absorption spectrometry.
952 *Geostand. Newsl.* **25**, 127-132.

953 Trinquier A., Birck J.-L. and Allègre C. J. (2007) Widespread ⁵⁴Cr heterogeneity in the inner
954 solar system. *Astrophys. J.* **655**, 1179-1185.

955 Vollstaedt H., Mezger K. and Leya I. (2016) The isotope composition of selenium in
956 chondrites constrains the depletion mechanism of volatile elements in solar system
957 materials. *Earth Planet. Sci. Lett.* **450**, 372-380.

958 Wang Z. and Becker H. (2013) Ratios of S, Se and Te in the silicate Earth require a volatile-
959 rich late veneer. *Nature* **499**, 328-331.

960 Wang Z., Becker H. and Wombacher F. (2015) Mass fractions of S, Cu, Se, Mo, Ag, Cd, In,
961 Te, Ba, Sm, W, Tl and Bi in geological reference materials and selected carbonaceous
962 chondrites determined by isotope dilution ICP-MS. *Geostand. Geoanal. Res.* **39**, 185-
963 208.

964 Wolf R., Richter G. R., Woodrow A. B. and Anders E. (1980) Chemical fractionations in
965 meteorites-XI. C2 chondrites. *Geochim. Cosmochim. Acta* **44**, 711-717.

966 Wolf S. F. and Lipschutz M. E. (1998) Chemical studies of H chondrites 9: Volatile trace
967 element composition and petrographic classification of equilibrated H chondrites.
968 *Meteorit. Planet. Sci.* **33**, 303-312.

969 Wombacher F., Rehkämper M., Mezger K., Bischoff A. and Münker C. (2008) Cadmium
970 stable isotope cosmochemistry. *Geochim. Cosmochim. Acta* **72**, 646-667.

971 Wombacher F., Rehkämper M., Mezger K. and Münker C. (2003) Stable isotope
972 compositions of cadmium in geological materials and meteorites determined by
973 multiple-collector ICPMS. *Geochim. Cosmochim. Acta* **67**, 4639-4654.

974 Wood B. J., Walter M. J. and Wade J. (2006) Accretion of the Earth and segregation of
975 its core. *Nature* **441**, 825-833.

976 Xiao X. and Lipschutz M. E. (1992) Labile trace-elements in carbonaceous chondrites - A
977 survey. *J. Geophys. Res. - Planets* **97**, 10199-10211.

978 Yi W., Halliday A. N., Alt J. C., Lee D.-C. and Rehkämper M. (2000) Cadmium, indium, tin,
979 tellurium, and sulfur in oceanic basalts: Implications for chalcophile element
980 fractionation in the Earth. *J. Geophys. Res.* **105**, 18927-18948.

981 Zanda B. (2004) Chondrules. *Earth Planet. Sci. Lett.* **224**, 1-17.

982 Zanda B., Bouret-Denise M., Perron C. and Hewins R. H. (1994) Origin and metamorphic
983 redistribution of silicon, chromium, and phosphorus in the metal of chondrites.
984 *Science* **265**, 1846-1849.

985 Zolensky M. E., Mittlefehldt D. W., Lipschutz M. E., Wang M.-S., Clayton R. N., Mayeda T.
986 K., Grady M. M., Pillinger C. and Barber D. (1997) CM chondrites exhibit the
987 complete petrologic range from type 2 to 1. *Geochim. Cosmochim. Acta* **61**, 5099-
988 5115.

989
990
991
992
993
994

995 **FIGURE CAPTIONS**

996

997 Fig. 1. Propagation of uncertainties of $\delta^{130/125}\text{Te}$ in relation of the spike proportion in the
998 spike-sample mixture.

999

1000 Fig 2. $\delta^{130/125}\text{Te}$ and Te concentration data for terrestrial samples. Closed symbols: sediment
1001 samples, open symbols: USGS geochemical exploration reference samples. Uncertainties for
1002 Te concentrations are smaller than symbols. For $\delta^{130/125}\text{Te}$ displayed errors are 2 SD of repeat
1003 analyses (see Tables 1, 2). For single analyses the uncertainty is the daily reproducibility (2
1004 SD) of the standard.

1005

1006 Fig. 3. $\delta^{130/125}\text{Te}$ data for chondritic meteorites, terrestrial samples and standard solutions (see
1007 Tables 1, 2). Panel a) all chondrite data, b) all data beside Mezö-Madaras (L3.7) and Dhajala
1008 (H3.8). Uncertainties for individual analyses are the daily reproducibility (2 SD) of the
1009 standard. For standard solutions, uncertainties are 2 SD of repeat analyses. Different symbols
1010 reflect different sample digestions. The grey area marks the composition of the terrestrial
1011 data.

1012

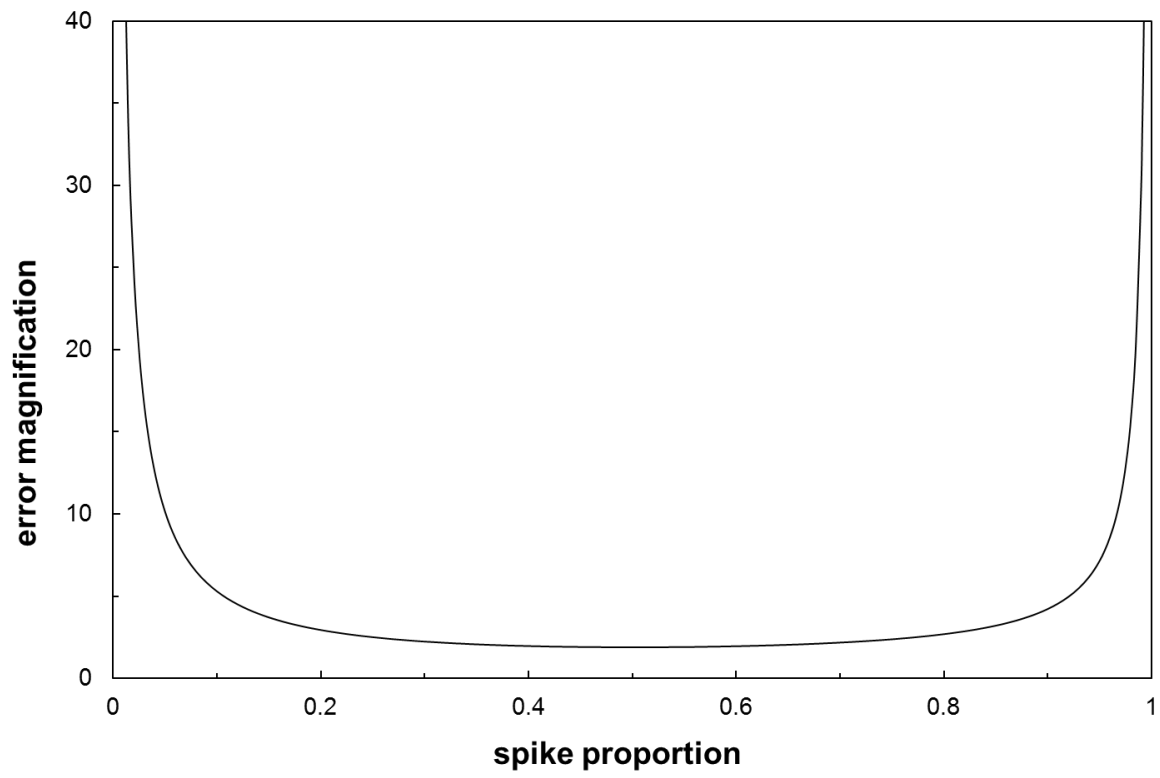
1013 Fig. 4. Tellurium stable isotope fractionation data and Te concentrations for chondrites. Panel
1014 a) ordinary chondrite data, b) all data beside Mezö-Madaras (L3.7) and Dhajala (H3.8).
1015 Uncertainties for Te concentrations are smaller than symbols, errors for $\delta^{130/125}\text{Te}$ are 2 SD of
1016 repeat analyses (Table 1). For single analyses uncertainties are the daily reproducibility (2
1017 SD) of the standard.

1018

1019

1020

1021



1022

1023

1024

1025

1026

1027

1028 Fig. 1

1029

1030

1031

1032

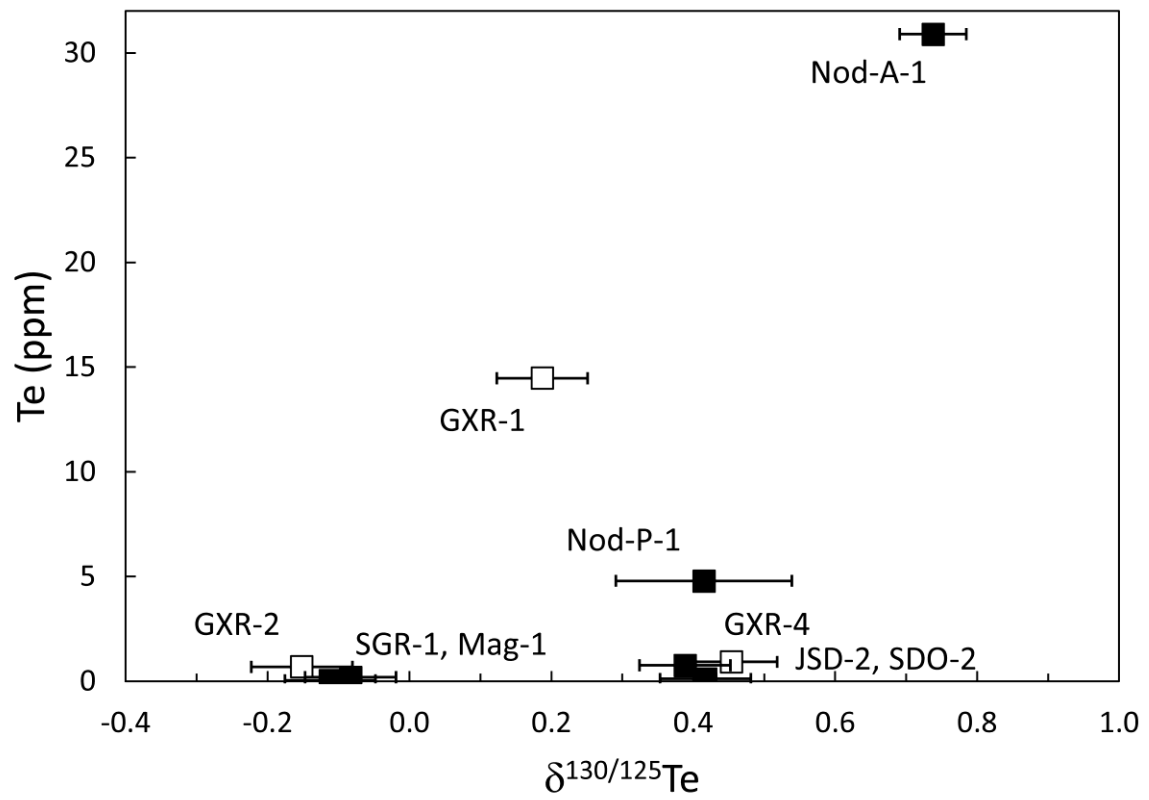
1033

1034

1035

1036

1037



1038

1039 Fig. 2

1040

1041

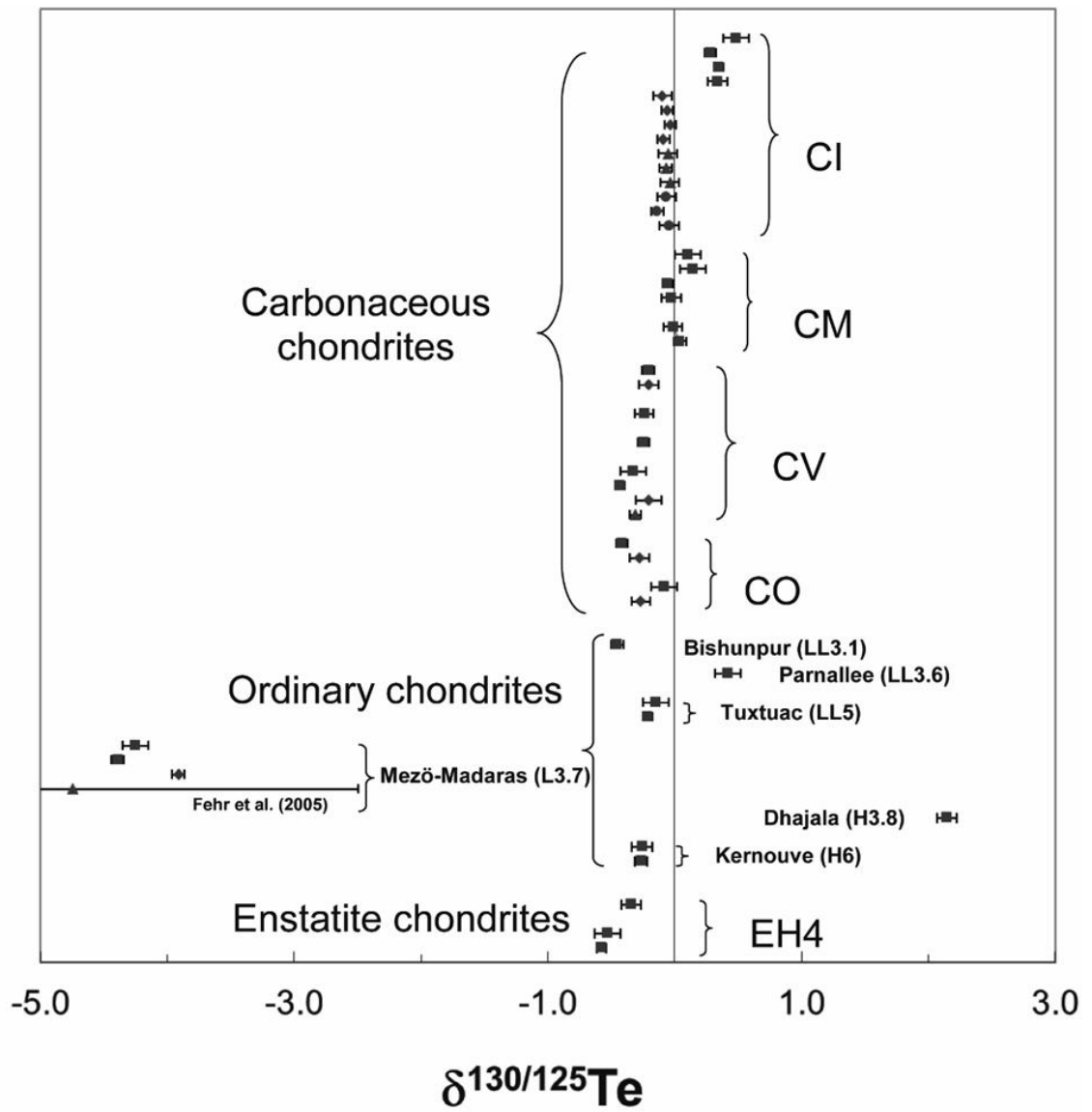
1042

1043

1044

1045

1046



1047

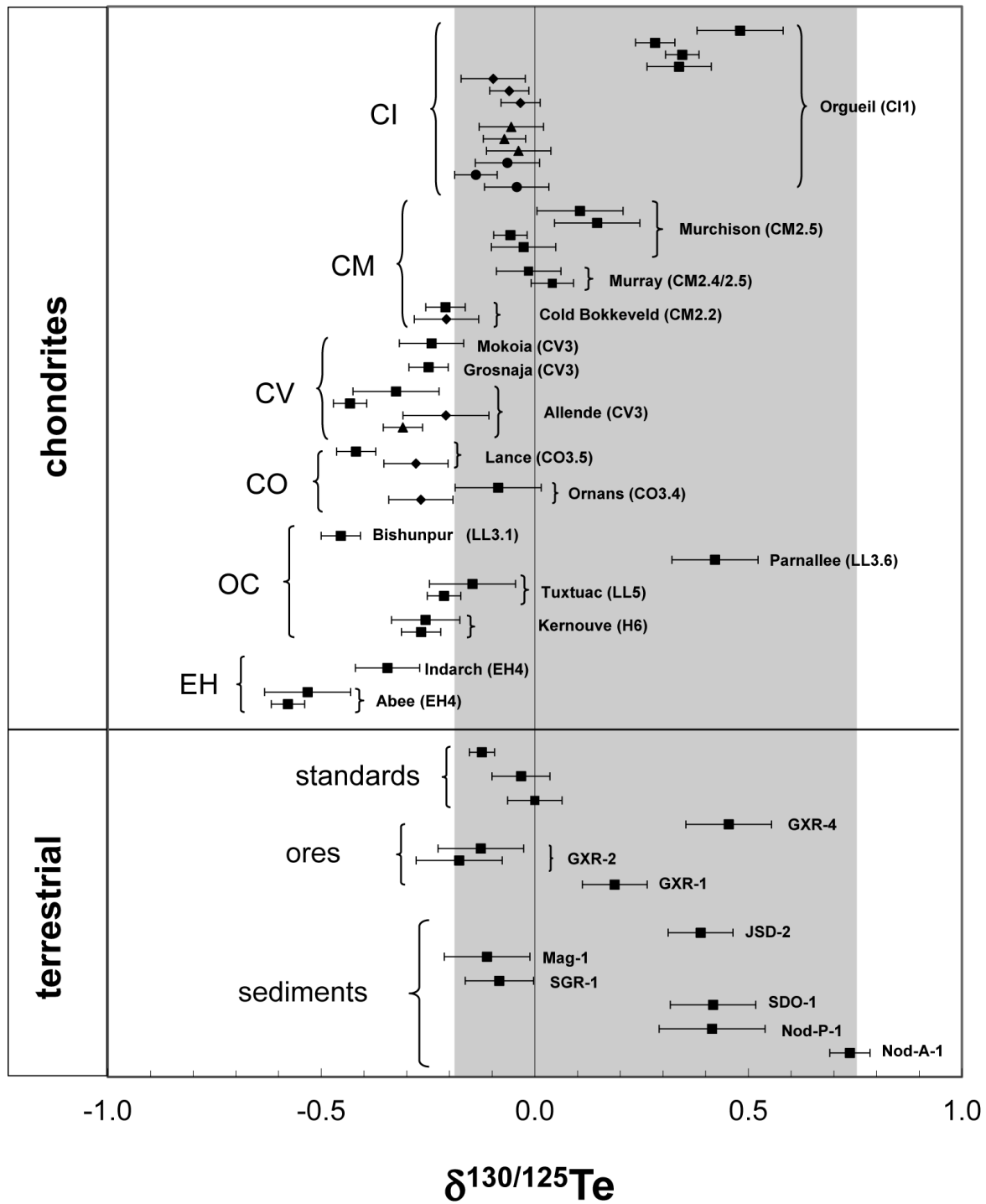
1048

1049 Fig. 3a

1050

1051

1052



1053

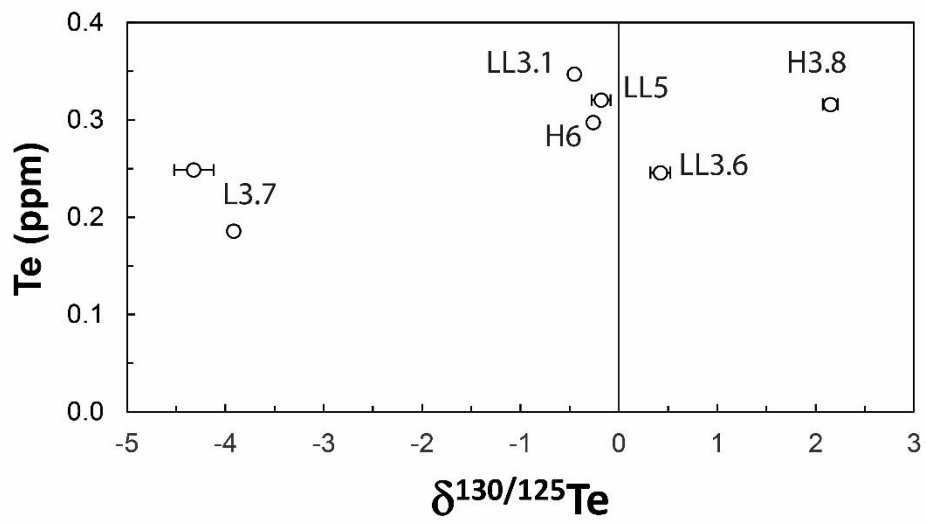
1054 Fig. 3b

1055

1056

1057

1058



1059

1060 Fig. 4a

1061

1062

1063

1064

1065

1066

1067

1068

1069

1070

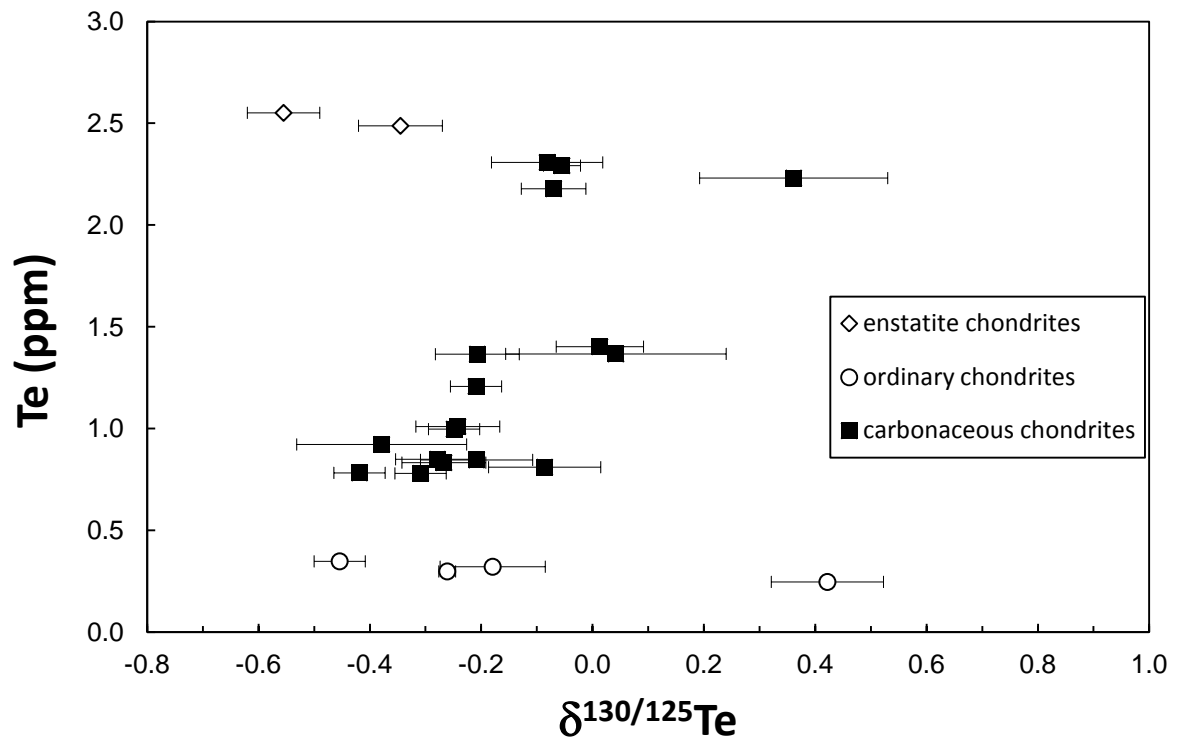
1071

1072

1073

1074

1075



1076
1077

1078

1079 Fig. 4b

1080

1081

1082

1083

1084

1085

1086

1087

1088

1089

1090

1091

Table 1: $\delta^{130/125}\text{Te}$ Te stable isotope data of terrestrial samples and standards and Te concentration data

Sample name	Supplier	Description	# ^a	$\delta^{130/125}\text{Te}$ ^b	2SD ^c	Te (ppm) ^d	Te (ppm) literature
Nod-A-1			rep. 1	0.72			
			rep. 2	0.73			
			rep. 3 ⁱ	0.76			
Mean Nod-A-1	USGS	Manganese nodule, Atlantic ocean	3	0.74	0.05	n.d.	30.9 ^e
Nod-P-1			rep. 1 ⁱ	0.36			
			rep. 2 ⁱ	0.33			
			rep. 3	0.39			
			rep. 4	0.48			
			rep. 5	0.47			
			rep. 6	0.45			
Mean Nod-P-1	USGS	Manganese nodule, Pacific ocean	6	0.42	0.12	n.d.	4.8 ^e
SDO-1	USGS	devonian Ohio shale		0.42	0.10	0.12	
SGR-1	USGS	green river shale		-0.08	0.08	0.20	0.23 ^f
Mag-1	USGS	marine mud, Gulf of Maine, Atlantic		-0.11	0.10	0.05	0.07 ^g
JSD-2	GSJ	stream sediment		0.39	0.08	0.77	0.8 ^h
GXR-1	USGS	jasperoid, Drum mountains, Utah		0.19	0.08	14.5	16 ^h
GXR-2			rep. 1	-0.18		0.69	
			rep. 2	-0.13		0.69	
Mean GXR -2	USGS	soil, Park City, Utah	2	-0.15	0.07	0.69	0.75 ^h
GXR-4	USGS	porphyry copper mill heads, Utah		0.45	0.10	0.93	1.06 ^h
Standards solutions							
Mean Te Alfa Aesar metal standard			154	0.00	0.06		
Mean Te standard SRM 3156			9	-0.12	0.03		
Te Alfa Aesar solution standard			2	-0.03	0.07		
Column processed standard							
300 ng Te -1			rep. 1	0.09			
			rep. 2	0.09			
			rep. 3	0.09			
			rep. 4	0.09			
Mean 300 ng Te -1		Te Alfa Aesar metal	4	0.09	0.00		
300 ng -2		Te Alfa Aesar metal		0.11	0.08		
50 ng Te		Te Alfa Aesar metal		0.02	0.08		
Mean Te		Te Alfa Aesar metal	3	0.07	0.10		

Te double spike was added after sample digestion

^a number of individual analyses: total number of repeat measurements (rep.)

^b $\delta^{130}\text{Te}/^{125}\text{Te} = [(^{130}\text{Te}/^{125}\text{Te}_{\text{sample}} / ^{130}\text{Te}/^{125}\text{Te}_{\text{alfa aesar metal}}) - 1] \times 1000$

^c 2SD reproducibility of daily standards shown for single analyses

^d 2SE of single analyses and 2SD of repeat analyses are <0.001 ppm and are not displayed.

^e Axelsson et al. (2002) ^f Hall ^g Wang et al. (2015) ^h Terashima (2001)

ⁱ Analysis performed using standard skimmer cone

1093

1094

1095

1096

1097

1098

Table 2: $\delta^{130/125}\text{Te}$ Te stable isotope fractionation and Te concentration data of chondrites

Sample name	Classification	Specimen	Shock	# ^a	$\delta^{130/125}\text{Te}^b$	2SD ^c	Te (ppm)	2SD ^d	Te (ppm) literature		
Orgueil	CI				diss. 1, rep. 1	0.48	2.23				
					diss. 1, rep. 2	0.28	2.23				
					diss. 1, rep. 3	0.35	2.23				
					diss. 1, rep. 4	0.34	2.23				
					Mean diss. 1 ^e	4	0.36			0.17	2.23
					diss. 2, rep. 1	-0.10	2.18				
					diss. 2, rep. 2	-0.06	2.18				
					diss. 2, rep. 3	-0.03	2.18				
					diss. 2, rep. 4	-0.09	2.18				
					Mean diss. 2	4	-0.07			0.06	2.18
					diss. 3, rep. 1	-0.06	2.29				
					diss. 3, rep. 2	-0.07	2.29				
					diss. 3, rep. 3	-0.04	2.29				
					Mean diss. 3 ^e	3	-0.05			0.03	2.29
					diss. 4, rep. 1	-0.06	2.31				
					diss. 4, rep. 2	-0.14	2.31				
diss. 4, rep. 3	-0.04	2.31									
Mean diss. 4 ^e	3	-0.08	0.10	2.31							
Mean, Orgueil	CI			4	0.04	0.42	2.25	0.12	2.3 - 2.6 ⁱ		
Cold Bokkeveld	CM2.2	BM82818			diss. 1	-0.21	0.05	1.21			
		BM82818			diss. 2 ^e	-0.21	0.08	1.37			
Mean Cold Bokkeveld	CM2.2		S1	2	-0.21	0.00	1.29	0.22	1.1 ⁱ - 1.3 ^k		
Murray	CM 2.4/2.5	BM1971, 288			rep. 1	-0.01		1.40			
					rep. 2	0.04		1.40			
Mean Murray	CM 2.4/2.5		S1		^e	0.01	0.08	1.40	1.4 ^l		
Murchison	CM2.5	1988.M23			rep. 1	0.11		1.37			
					rep. 2	0.15		1.37			
					rep. 3	-0.06		1.37			
					rep. 4	-0.03		1.36			
Mean Murchison	CM2.5		S1-2	4	0.04	0.20	1.37		1.3-1.8 ^{f,i,l}		
Ormans	CO3.4	BM1920, 329			diss. 1	-0.09	0.10	0.81			
		BM1920, 329			diss. 2 ^e	-0.27	0.08	0.83			
Mean Ormans	CO3.4		S1	2	-0.18	0.26	0.82	0.03	1 ^m		
Lance	CO3.5	BM1985, M153			diss. 1	-0.42	0.05	0.78			
		BM1985, M153			diss. 2 ^e	-0.28	0.08	0.85			
Mean Lance	CO3.5		S1	2	-0.35	0.20	0.81	0.09	0.84 ⁿ		
Allende	CV3	BM1969, 148			diss. 1, rep. 1	-0.32		0.92			
					diss. 1, rep. 2	-0.43		0.92			
					Mean diss. 1 ^e	2	-0.38	0.15	0.92		
		BM1969, 148			diss. 2	-0.21	0.10	0.85			
		BM1969, 148			diss. 3	-0.31	0.05	0.78			
Mean Allende	CV3		S1	3	-0.30	0.17	0.85	0.14	0.86 - 1.1 ^{f,h,i,o}		

Table 2 continued

Sample name	Classification	Specimen	Shock	# ^a	$\delta^{130/125}\text{Te}^b$	2SD ^c	Te (ppm)	2SD ^d	Te (ppm) literature
Grosnaja	CV3	63624	S3		-0.25	0.05	1.00		1.2 ⁿ
Mokoia	CV3	BM 1910.729	S1	^e	-0.24	0.08	1.01		1 ⁿ
Parnallee	LL3.6	BM34792	b		0.42	0.10	0.25		0.2 ^p
Bishunpur	LL3.1	BM80339	S2		-0.45	0.05	0.35		0.5 ^p
Tuxtuac	LL5	BM1981, M7		rep. 1	-0.15		0.32		
				rep. 2	-0.21		0.32		
Mean Tuxtuac	LL5	BM1981, M7	S2	^e	2	-0.18	0.09	0.32	
Mezö-Madaras	L3.7	BM90270		diss. 1, rep. 1	-4.25		0.25		
				diss. 1, rep. 2	-4.39		0.25		
				Mean diss. 1 ^e	2	-4.32	0.20	0.25	
		BM90270		diss. 2	-3.91	0.05	0.19		
Mean Mezö-Madaras	L3.7		b		2	-4.12	0.58	0.22	0.09
									0.57 ⁱ - 0.88 ^q
Dhajala	H3.8	BM1976, M12	S1	^e	2.15	0.08	0.32		
Kernouve	H6	BM43400		rep. 1	-0.26		0.30		
				rep. 2	-0.27		0.30		
Mean Kernouve	H6		S1		2	-0.26	0.02	0.30	
									0.34 ^r - 0.38 ^s
Abee	EH4	BM1992, M7		rep. 1	-0.53		2.55		
				rep. 2	-0.58		2.55		
Mean Abee	EH4		S2-4	^e	2	-0.55	0.07	2.55	
									1.7 ⁱ - 3 ⁱ
Indarch	EH4	BM86948	S3	^e	-0.34	0.08	2.49		2 ⁱ

^a number of individual analyses: total number of repeat measurements (rep.) of one or several separate sample dissolutions (diss.)

^b $\delta^{130}\text{Te}/^{125}\text{Te} = [({}^{130}\text{Te}/^{125}\text{Te}_{\text{sample}} / {}^{130}\text{Te}/^{125}\text{Te}_{\text{alpha aesar metal}}) - 1] \times 1000$

^c 2SD reproducibility of daily standards shown for single analyses

^d 2SD of repeat analyses are <0.002 ppm and are not displayed

^e Te double spike was added before sample digestion

Literature data are from ^f Smith et al. (1977), ^g Xiao and Lipschutz (1992), ^h Friedrich et al. (2002), ⁱ Fehr et al. (2005), ^j Wolf et al. (1980),

^k Zolensky et al. (1997), ^l Makishima and Nakamura (2009), ^m Takahashi et al. (1978), ⁿ Anders et al. (1976), ^o Wang et al. (2015),

^p Binz et al. (1976), ^q Keays et al. (1971), ^r Morgan et al. (1985), ^s Lingner et al. (1978), ^t Kallemeyn and Wasson (1986)